Contents

Part IV

ELASTICITY

Chapter 11

Elastostatics

Version 1011.1.K, 14 January 2009.
Please send comments, suggestions, and errata via email to kip@caltech.edu or on paper to Kip Thorne, 350-17 Caltech, Pasadena CA 91125

Box 11.1
Reader's Guide

- This chapter relies heavily on the geometric view of Newtonian physics (including vector and tensor analysis) laid out in the sections of Chap. 1 labeled "[N]".
- Chapter 11 (Elastodynamics) is an extension of this chapter; to understand it, this chapter must be mastered.
- The idea of the *irreducible tensorial parts* of a tensor, and its most important example, decomposition of the strain tensor into expansion, rotation, and shear (Sec. 11.2.2 and Box 11.2) will be encountered again in Part IV (Fluid Mechanics) and Part V (Plasma Physics).
- Differentiation of vectors and tensors with the help of *connection coefficients* (Sec. 11.5), will be used occasionally in Part IV (Fluid Mechanics) and Part V (Plasma Physics), and will be generalized to non-orthonormal bases in Part VI (General Relativity) and used extensively there.
- No other portions of this chapter are important for subsequent Parts of this book.

11.1 Overview

In this chapter we consider static equilibria of elastic solids — for example, the equilibrium shape and internal strains of a cantilevered balcony on a building, deformed by the weight of people standing on it.

From the point of view of continuum mechanics, a *solid* (e.g. a wooden board in the balcony) is a substance that recovers its shape after the application and removal of *any* small stress. In other words, after the stress is removed, the solid can be rotated and translated to assume its original shape. Note the requirement that this be true for any stress. Many fluids (e.g. water) satisfy our definition as long as the applied stress is isotropic; however, they will deform permanently under a shear stress. Other materials (for example, the earth's crust) are only elastic for limited times, but undergo plastic flow when a stress is applied for a long time.

We shall confine our attention in this chapter to *elastic solids*, which deform while the stress is applied in such a way that the magnitude of the deformation (quantified by a *tensorial strain*) is linearly proportional to the applied, *tensorial stress*. This linear, three-dimensional stress-strain relationship, which we shall develop and explore in this chapter, generalizes Hooke's famous one-dimensional law (originally expressed in the concise Latin phrase "*Ut tensio, sic vis*"). In English, Hooke's law says that, if an elastic wire or rod is stretched by an applied force F (Fig. 11.1a), its fractional change of length (its strain) is proportional to the force, $\Delta\ell/\ell \propto F$. In the language of stresses and strains (introduced below), Hooke's law says that the longitudinal stress $T_{zz} \equiv$ (longitudinal force F per unit cross sectional area A of the rod) $= F/A$ is proportional to the longitudinal strain $S_{zz} = \Delta\ell/\ell$, with a proportionality constant E called *Young's modulus* that is a property of the material from which the rod is made:

$$\frac{F}{A} \equiv T_{zz} = ES_{zz} \equiv E\frac{\Delta\ell}{\ell} \ . \tag{11.1}$$

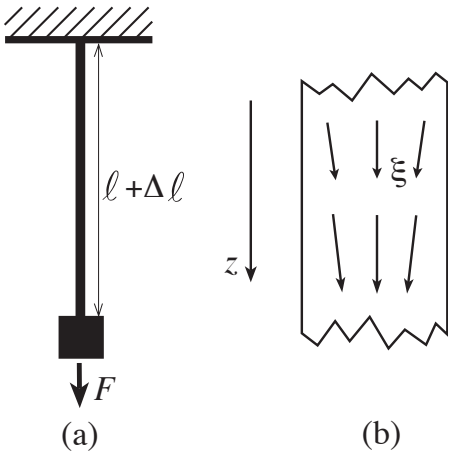

Fig. 11.1: (a) Hooke's one-dimensional law for a rod stretched by a force F: $\Delta\ell/\ell \propto F$. (b) The 3-dimensional displacement vector $\boldsymbol{\xi}(\mathbf{x})$ inside the stretched rod.

Hooke's law will turn out to be one component of the three-dimensional stress-strain relation, but in order to understand it deeply in that language, we must first develop a deep understanding of the strain tensor and the stress tensor. Our approach to these tensors will follow the geometric, frame-independent philosophy introduced in Chap. 1. Some readers

may wish to review that philosophy and associated mathematics by rereading the "[N]" sections of Chap. 1.

We begin in Sec. 11.2 by introducing, in a frame-independent way, the vectorial displacement field $\boldsymbol{\xi}(\mathbf{x})$ inside a stressed body and its gradient $\boldsymbol{\nabla}\boldsymbol{\xi}$, which is the strain tensor $\mathbf{S} = \boldsymbol{\nabla}\boldsymbol{\xi}$. We then express the strain tensor as the sum of its *irreducible tensorial parts*: an *expansion* Θ, a *rotation* $\mathbf{R}$, and a *shear* $\boldsymbol{\Sigma}$.

In Sec. 11.3.1 we introduce the stress tensor for a deformed, isotropic, elastic material. In Sec. 11.3.2, we discuss how such a material resists volume change (an expansion-type strain) by developing an opposing isotropic stress, with a stress/strain ratio that is equal to the *bulk modulus* K; and how the material also resists a shear-type strain by developing an opposing shear stress with a stress/strain ratio equal to twice the *shear modulus* 2μ. We then compute the elastic force density inside the material, as the divergence of the sum of these two elastic stresses, and we formulate the law of *elastostatic stress balance* as the vanishing sum of the material's internal elastic force density and any other force densities that may act (usually a gravitational force density due to the weight of the elastic material). We discuss the analogy between this elastostatic stress-balance equation and Maxwell's electrostatic or magnetostatic equations, and we describe how mathematical techniques common in electrostatics (separation of variables and Green's functions) can also be applied to solve the elastostatic stress-balance equation, subject to boundary conditions that describe external forces (e.g. the pressure of a person's feet, standing on a balcony). In Sec. 11.3.3 we evaluate the energy density stored in elastostatic strains, and in Sec. 11.3.4 we discuss the atomic-force origin of the elastostatic stresses and use atomic considerations to estimate the magnitudes of the bulk and shear moduli.

In Sec. 11.4 we present a simple example of how to solve the three-dimensional equation of elastostatic force balance subject to the appropriate boundary conditions on the surface of a stressed body. Specficially, we use our three-dimensional formulas to deduce Hooke's law for the one-dimensional longitudinal stress and strain in a stretched wire, and we thereby relate Young's modulus E of Hooke's law to the bulk modulus K that resists three-dimensional volume changes, and the shear modulus μ that resists three-dimensional shears.

Because elasticity theory entails computing gradients of vectors and tensors, and practical calculations are often best performed in cylindrical or spherical coordinate systems, we present a mathematical digression in Sec. 11.5 — an introduction to how one can perform practical calculations of gradients of vectors and tensors in the orthonormal bases associated with curvilinear coordinate systems, using the concept of a *connection coefficient* (the directional derivative of one basis vector field along another). In Sec. 11.5 we also use these connection coefficients to derive some useful differentiation formulae in cylindrical and spherical coordinate systems and bases.

As illustrative examples of both connection coefficients and elastostatic force balance, in Sec 11.6 and various exercises, we give practical examples of solutions of the elastostatic force-balance equation in cylindrical coordinates: for the stresses and strains in a pipe that contains a fluid under pressure (Sec. 11.6.1 and Ex. 11.11) and in the wire of a torsion pendulum (Ex. 11.12); and in a cylinder that is subjected to a Gaussian-shaped pressure on one face (Sec. 11.6.2). As we shall see in Ex. 11.14, this cylinder-pressure problem is one part of computing the spectral density of thermoelastic noise inside the test-mass mirrors of

a gravitational-wave interferometer — an application of the fluctuation-dissipation theorem that we introduced and discussed in Sec. 5.6 and Ex. 5.8 of Chap. 5 (Random Processes). We shall sketch how to solve this cylinder-pressure problem using the two common techniques of elastostatics and electrostatics: separation of variables (text of Sec. 11.6.2) and a Green's function (Ex. 11.15)

When the elastic body that one studies is very thin in two dimensions compared to the third (e.g., a wire or rod), we can reduce the three-dimensional elastostatic equations to a set of coupled one-dimensional equations by performing a two-lengthscale expansion. The key to this *dimensional reduction* is taking *moments* of the elastostatic equations. We illustrate this technique in Sec. 11.7, where we treat the bending of beams (e.g. for a cantilevered balcony or bridge), and in exercises where we treat the bending of the support wire of a Foucault pendulum, and the bending of a very long, thin wire to which forces are applied at the ends (*elastica*).

Elasticity theory, as developed in this chapter, is an example of a common (some would complain far too common) approach to physics problems, namely to linearize them. Linearization may be acceptable when the distortions are small. However, when deformed by sufficiently strong forces, elastic media may become neutrally stable to small displacements, which can then grow to large amplitude. We shall study an example of this phenomenon in Sec. 11.8, using our dimensionally reduced, one-dimensional theory. Our example will lead us to a classic result, due originally to Euler: that when an elastic solid is compressed, there comes a point where stable equilibria can disappear altogether. For an applied force in excess of this maximum, the solid will *buckle*, a phenomenon that gives rise, in the earth's crust, to mountains (as we shall discuss). Buckling is associated with *bifurcation of equilibria*, a phenomenon that is common to many physical systems, not just elastostatic ones. We illustrate bifurcation in Sec. 11.8 using a strut under a compressive load, and we will encounter bifurcation again in Sec. 14.5, when we study the route to turbulence in fluids and the route to chaos in other dynamical systems.

Finally, in Sec. 11.9 we discuss dimensional reduction by the method of moments for bodies that are thin in only one dimension, not two; e.g. plates and thin mirrors. In this case the three-dimensional elastostatic equations are reduced to two dimensions. We illustrate our two-dimensional formalism by the stress polishing of telescope mirrors.

11.2 Displacement and Strain; Expansion, Rotation, and Shear

We begin our study of elastostatics by introducing the elastic displacement vector, its gradient (the strain tensor), and the irreducible tensorial parts of the strain.

11.2.1 Displacement Vector and Strain Tensor

We label the position of a *point* (a tiny bit of solid) in an unstressed body, relative to some convenient origin in the body, by its position vector $\mathbf{x}$. Let a force be applied so the body deforms and the point moves from $\mathbf{x}$ to $\mathbf{x} + \boldsymbol{\xi}(\mathbf{x})$; we call $\boldsymbol{\xi}$ the point's *displacement vector*.

If $\boldsymbol{\xi}$ were constant (i.e., if its components in a Cartesian coordinate system were independent of location in the body), then the body would simply be translated and would undergo no deformation. To produce a deformation, we must make the displacement $\boldsymbol{\xi}$ change from one location to another. The most simple, *coordinate-independent* way to quantify those changes is by the *gradient* of $\boldsymbol{\xi}$, $\boldsymbol{\nabla\xi}$. This gradient is a second-rank tensor field;[1] we shall give it the name *strain tensor* and shall denote it $\mathbf{S}$:

$$\boxed{\mathbf{S} = \boldsymbol{\nabla\xi} \ .} \tag{11.2a}$$

This strain tensor is a geometric object, defined independent of any coordinate system in the manner described in Sec. 1.9. In slot-naming index notation (Sec. 1.5), it is denoted

$$S_{ij} = \xi_{i;j} \ , \tag{11.2b}$$

where the index j after the semicolon is the name of the gradient slot.

In a Cartesian coordinate system the components of the gradient are always just partial derivatives [Eq. (1.54c)], and therefore the Cartesian components of the strain tensor are

$$S_{ij} = \frac{\partial \xi_i}{\partial x_j} = \xi_{i,j} \ . \tag{11.2c}$$

(Recall that indices following a comma represent partial derivatives.) In the next section we shall learn how to compute the components of the strain in cylindrical and spherical coordinates.

For the one-dimensional Hooke's-Law situation of Fig. 11.1a, we have $\xi_z = z(\Delta\ell/\ell)$ and $S_{zz} = \xi_{z;z} = \partial\xi_z/\partial z = \Delta\ell/\ell$ [Eq. (11.1)]. If we look in greater detail at the interior of the stretched rod, paying attention to its three-dimensional structure, we see that the rod's resistance to volume changes causes it to shrink in cross section as it stretches in length. This shows up as an inward component of the displacement vector (Fig. 11.1b), so $S_{xx} = \partial\xi_x/\partial x < 0$, $S_{yy} = \partial\xi_y/\partial y < 0$, $S_{zz} = \partial\xi_z/\partial z > 0$.

In any small neighborhood of any point $\mathbf{x}_o$ in a deformed body, we can reconstruct the displacement vector $\boldsymbol{\xi}$ from the strain tensor, up to an additive constant. In Cartesian coordinates, by virtue of a Taylor-series expansion, $\boldsymbol{\xi}$ is given by

$$\begin{aligned} \xi_i(\mathbf{x}) &= \xi_i(\mathbf{x}_o) + (x_j - x_{oj})(\partial\xi_i/\partial x_j) + \dots \\ &= \xi_i(\mathbf{x}_o) + (x_j - x_{oj})S_{ij} + \dots \ . \end{aligned} \tag{11.3}$$

If we place our origin of Cartesian coordinates at $\mathbf{x}_o$ and let the origin move with the point there as the body deforms [so $\boldsymbol{\xi}(\mathbf{x}_o) = 0$], then Eq. (11.3) becomes

$$\xi_i = S_{ij}x_j \quad \text{when } |\mathbf{x}| \text{ is sufficiently small} \ . \tag{11.4}$$

We have derived this as a relationship between components of $\boldsymbol{\xi}$, $\mathbf{x}$, and $\mathbf{S}$ in a Cartesian coordinate system. However, the indices can also be thought of as the names of slots (Sec. 1.5) and correspondingly Eq. (11.4) can be regarded as a geometric, coordinate-independent relationship between the vectors and tensor $\boldsymbol{\xi}$, $\mathbf{x}$, and $\mathbf{S}$.

In Ex. 11.2 we shall use Eq. (11.4) to gain insight into the displacements associated with various types of strain.

[1] In our treatment of elasticity theory, we shall make extensive use of the tensorial concepts introduced in Chap. 1.

Box 11.2
Irreducible Tensorial Parts of a Second-Rank Tensor in 3-Dimensional Euclidean Space

In quantum mechanics an important role is played by the "rotation group," i.e., the set of all rotation matrices viewed as a mathematical entity called a group; see, e.g., chapter XIII of Messiah (1962) or chapter 16 of Mathews and Walker (1965). Each tensor in 3-dimensional Euclidean space, when rotated, is said to generate a specific "representation" of the rotation group. Tensors that are "big", in a sense to be discussed below, can be broken down into a sum of several tensors that are "as small as possible." These smallest tensors are said to generate "irreducible representations" of the rotation group. All this mumbo-jumbo is really very simple, when one thinks about tensors as geometric, frame-independent objects.

As an example, consider an arbitrary second-rank tensor S_{ij} in three-dimensional, Euclidean space. In the text S_{ij} is the strain tensor. From this tensor we can construct the following "smaller" tensors by linear operations that involve only S_{ij} and the metric g_{ij}. (As these smaller tensors are enumerated, the reader should think of the notation used as basis-independent, frame-independent, slot-naming index notation.) The smaller tensors are the "trace" of S_{ij},

$$\Theta \equiv S_{ij} g_{ij} = S_{ii} \ ; \tag{1}$$

the antisymmetric part of S_{ij}

$$R_{ij} \equiv \frac{1}{2}(S_{ij} - S_{ji}) \ ; \tag{2}$$

and the symmetric, trace-free part of S_{ij}

$$\Sigma_{ij} \equiv \frac{1}{2}(S_{ij} + S_{ji}) - \frac{1}{3} g_{ij} S_{kk} \ . \tag{3}$$

It is straightforward to verify that the original tensor S_{ij} can be reconstructed from these three "smaller" tensors, plus the metric g_{ij} as follows:

$$S_{ij} = \frac{1}{3}\Theta g_{ij} + \Sigma_{ij} + R_{ij} \ . \tag{4}$$

One way to see the sense in which Θ, R_{ij}, and Σ_{ij} are "smaller" than S_{ij} is by counting the number of independent real numbers required to specify their components in an arbitrary basis. (In this counting the reader is asked to think of the index notation as components on the chosen basis.) The original tensor S_{ij} has $3 \times 3 = 9$ components $(S_{11}, S_{12}, S_{13}, S_{21}, \ldots)$, all of which are independent. By contrast, the 9 components of Σ_{ij} are not independent; symmetry requires that $\Sigma_{ij} \equiv \Sigma_{ji}$, which reduces the number of independent components from 9 to 6; trace-freeness, $\Sigma_{ii} = 0$ reduces it further from 6 to 5. The antisymmetric tensor R_{ij} has just three independent components, R_{12}, R_{23},

Box 11.2, Continued

and R_{31}. The scalar Θ has just one. Therefore, (5 independent components in Σ_{ij}) + (3 independent components in R_{ij}) + (1 independent components in Θ) = 9 = (number of independent components in S_{ij}).

The number of independent components (one for Θ, 3 for R_{ij}, 5 for Σ_{ij}) is a geometric, basis-independent concept: It is the same, regardless of the basis used to count the components; and for each of the "smaller" tensors that make up S_{ij}, it is easily deduced without introducing a basis at all: (Here the reader is asked to think in slot-naming index notation.) The scalar Θ is clearly specified by just one real number. The antisymmetric tensor R_{ij} contains precisely the same amount of information as the vector

$$\phi_i \equiv -\frac{1}{2}\epsilon_{ijk}R_{jk} \ , \tag{5}$$

as one can see from the fact that Eq. (5) can be inverted to give

$$R_{ij} = -\epsilon_{ijk}\phi_k \ ; \tag{6}$$

and the vector ϕ_i can be characterized by its direction in space (two numbers) plus its length (a third). The symmetric, trace-free tensor Σ_{ij} can be characterized geometrically by the ellipsoid $(g_{ij}+\varepsilon\Sigma_{ij})\zeta_i\zeta_j = 1$, where ε is an arbitrary number $\ll 1$ and ζ_i is a vector whose tail sits at the center of the ellipsoid and head moves around on the ellipsoid's surface. Because Σ_{ij} is trace-free, this ellipsoid has unit volume. It therefore is specified fully by the direction of its longest principal axis (two numbers) plus the direction of a second principle axis (a third number) plus the ratio of the length of the second axis to the first (a fourth number) plus the ratio of the length of the third axis to the first (a fifth number).

Each of the tensors Θ, R_{ij} (or equivalently ϕ_i), and Σ_{ij} is "irreducible" in the sense that one cannot construct any "smaller" tensors from it, by any linear operation that involves only it, the metric, and the Levi-Civita tensor. Irreducible tensors in 3-dimensional Euclidean space always have an odd number of components. It is conventional to denote this number by $2l+1$ where the integer l is called the "order of the irreducible representation of the rotation group" that the tensor genenerates. For Θ, R_{ij} (or equivalently ϕ_i), and Σ_{jk}, l is 0, 1, and 2 respectively. These three tensors can be mapped into the spherical harmonics of order $l = 0,\ 1,\ 2$; and their $2l+1$ components correspond to the $2l+1$ values of the quantum number $m = -l,\ -l+1\ \ldots\ , l-1,\ l$. For details see, e.g., section II.C of Thorne (1980).

In physics, when one encounters a new, unfamiliar tensor, it is often useful to identify the tensor's irreducible parts. They almost always play important, independent roles in the physical situation one is studying. We meet one example in this chapter (the strain tensor), and shall meet another when we study fluid mechanics (Chap. 12).

11.2.2 Expansion, Rotation and Shear

In Box 11.2 we introduce the concept of the *irreducible tensorial parts* of a tensor, and we state that in physics, when one encounters a new, unfamiliar tensor, it is often useful to identify the tensor's irreducible parts. The strain tensor $\mathbf{S}$ is an important example. It is a general, second-rank tensor. Therefore, as we discuss in Box 11.2, its irreducible tensorial parts are its trace $\Theta \equiv \mathrm{Tr}(\mathbf{S}) = S_{ii} = \boldsymbol{\nabla}\cdot\boldsymbol{\xi}$, which is called the deformed body's *expansion* for reasons we shall explore below; its symmetric, trace-free part $\boldsymbol{\Sigma}$, which is called the body's *shear*; and its antisymmetric part $\mathbf{R}$, which is called the body's *rotation*:

$$\boxed{\Theta = S_{ii} = \boldsymbol{\nabla}\cdot\boldsymbol{\xi}\ ,} \tag{11.5a}$$

$$\boxed{\Sigma_{ij} = \frac{1}{2}(S_{ij}+S_{ji}) - \frac{1}{3}\Theta g_{ij} = \frac{1}{2}(\xi_{i;j}+\xi_{j;i}) - \frac{1}{3}\Theta g_{ij}\ ,} \tag{11.5b}$$

$$\boxed{R_{ij} = \frac{1}{2}(S_{ij}-S_{ji})\ .} \tag{11.5c}$$

Here g_{ij} is the metric, which has components $g_{ij} = \delta_{ij}$ (Kronecker delta) in Cartesian coordinates.

The strain tensor can be reconstructed from these irreducible tensorial parts in the following manner [Eq. (4) of Box 11.2, rewritten in abstract notation]:

$$\boxed{\boldsymbol{\nabla}\boldsymbol{\xi} = \mathbf{S} = \frac{1}{3}\Theta\mathbf{g} + \boldsymbol{\Sigma} + \mathbf{R}.} \tag{11.6}$$

Let us consider the physical effects of the three separate parts of $\mathbf{S}$ in turn. To understand expansion, consider a small 3-dimensional piece $\mathcal{V}$ of a deformed body (a "volume element"). An element of area[2] $d\boldsymbol{\Sigma}$ on the surface $\partial\mathcal{V}$ of $\mathcal{V}$ gets displaced through a vectorial distance $\boldsymbol{\xi}$ and in the process sweeps out a volume $\boldsymbol{\xi}\cdot d\boldsymbol{\Sigma}$. Therefore, the change in the volume element's volume, produced by an arbitrary (small) displacement field $\boldsymbol{\xi}$ is

$$\delta V = \int_{\partial\mathcal{V}} d\boldsymbol{\Sigma}\cdot\boldsymbol{\xi} = \int_{\mathcal{V}} dV\,\boldsymbol{\nabla}\cdot\boldsymbol{\xi} = \boldsymbol{\nabla}\cdot\boldsymbol{\xi}\int_{\mathcal{V}} dV = (\boldsymbol{\nabla}\cdot\boldsymbol{\xi})V\ . \tag{11.7}$$

Here we have invoked Gauss' theorem in the second equality, and in the third we have used the smallness of $\mathcal{V}$ to infer that $\boldsymbol{\nabla}\cdot\boldsymbol{\xi}$ is essentially constant throughout $\mathcal{V}$ and so can be pulled out of the integral. Therefore, the fractional change in volume is equal to the trace of the stress tensor, i.e. the expansion:

$$\boxed{\frac{\delta V}{V} = \boldsymbol{\nabla}\cdot\boldsymbol{\xi} = \Theta\ .} \tag{11.8}$$

See Figure 11.2 for a simple example.

The shear tensor $\boldsymbol{\Sigma}$ produces the shearing displacements illustrated in Figures 11.2 and 11.3. As it has zero trace, there is no volume change when a body undergoes a pure shear

[2]Note that we use $\boldsymbol{\Sigma}$ for a vectorial area and $\boldsymbol{\Sigma}$ for a strain tensor. There should be no confusion.

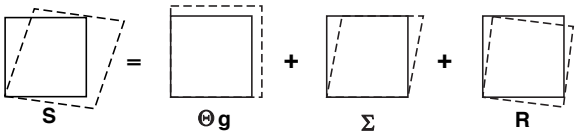

Fig. 11.2: A simple example of the decomposition of a two dimensional distortion of a square body into an expansion (Θ), a shear ($\mathbf{\Sigma}$), and a rotation ($\mathbf{R}$).

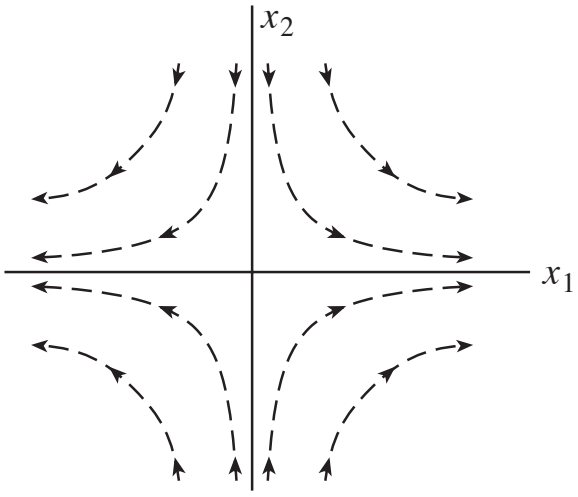

Fig. 11.3: Shear in two dimensions. The displacement of points in a solid undergoing pure shear is the vector field $\boldsymbol{\xi}(\mathbf{x})$ given by Eq. (11.4) with S_{ji} replaced by Σ_{ji}: $\xi_j = \Sigma_{ji}x_i = \Sigma_{j1}x_1 + \Sigma_{j2}x_2$. The integral curves of this vector field are plotted in this figure. The figure is drawn using principal axes, which are Cartesian, so $\Sigma_{12} = \Sigma_{21} = 0$, $\Sigma_{11} = -\Sigma_{22}$, which means that $\xi_1 = \Sigma_{11}x_1$, and $\xi_2 = -\Sigma_{11}x_2$. The integral curves of this simple vector field are the hyperbolae shown in the figure. Note that the displacement increases linearly with distance from the origin.

deformation. The shear tensor has five independent components (Box 11.2). However, by rotating our Cartesian coordinates appropriately, we can transform away all the off diagonal elements, leaving the three diagonal elements, which must sum to zero. This is known as a *principal axis transformation*. The components of the shear tensor in a cartesian coordinate system can be written down immediately from Eq. (11.5b) by substituting the Kronecker delta δ_{ij} for the components of the metric tensor g_{ij} and treating all derivatives as partial derivatives:

$$\Sigma_{xx} = \frac{2}{3}\frac{\partial \xi_x}{\partial x} - \frac{1}{3}\left(\frac{\partial \xi_y}{\partial y} + \frac{\partial \xi_z}{\partial z}\right) \ , \quad \Sigma_{xy} = \frac{1}{2}\left(\frac{\partial \xi_x}{\partial y} + \frac{\partial \xi_y}{\partial x}\right) \ , \tag{11.9}$$

and similarly for the other components. The analogous equations in spherical and cylindrical coordinates will be described in the next section.

The third term in Eq. (11.6) describes a pure rotation which does not deform the solid. To verify this, write $\boldsymbol{\xi} = \boldsymbol{\phi} \times \mathbf{x}$ where $\boldsymbol{\phi}$ is a small rotation of magnitude ϕ about an axis parallel to the direction of $\boldsymbol{\phi}$. Using cartesian coordinates in three dimensional Euclidean space, we can demonstrate by direct calculation that the symmetric part of $\mathbf{S}$ vanishes, i.e.,

$\Theta = \mathbf{\Sigma} = 0$ and that

$$R_{ij} = -\epsilon_{ijk}\phi_k \ , \qquad \phi_i = -\frac{1}{2}\epsilon_{ijk}R_{jk} \ . \tag{11.10a}$$

Therefore the elements of the tensor $\mathbf{R}$ in a cartesian coordinate system just involve the angle $\boldsymbol{\phi}$. Note that expression (11.10a) for $\boldsymbol{\phi}$ and expression (11.5c) for R_{ij} imply that $\boldsymbol{\phi}$ is half the curl of the displacement vector,

$$\boldsymbol{\phi} = \frac{1}{2}\boldsymbol{\nabla} \times \boldsymbol{\xi} \ . \tag{11.10b}$$

A simple example of rotation is shown in the last picture in Figure 11.2.

Let us consider some examples of strains that can arise in physical systems.

(i) Understanding how materials deform under various loads is central to mechanical, civil and structural engineering. As we have already remarked, in an elastic solid, the deformation (i.e. strain) is proportional to the applied stress. If, for example, we have some structure of negligible weight and it supports a load, then the amount of strain will increase everywhere in proportion to this load. However this law will only be obeyed as long as the strain is sufficiently small that the material out of which the structure is constructed behaves elastically. At a large enough strain, *plastic flow* will set in and the solid will not return to its original shape after the stress is removed. The point where this happens is known as the *elastic limit*. For a *ductile* substance like polycrystalline copper with a relatively low elastic limit, this occurs at strains $\sim 10^{-4}$. [However, *failure* (cracking or breaking of the material) will not occur until the *yield point* which occurs at a strain $\sim 10^{-3}$.] For a more resilient material like cemented tungsten carbide, strains can be elastic up to $\sim 3\times10^{-3}$, and for rubber, a non-Hookean material, recoverable strains of three or four are possible. What is significant is that all these strains (with the exception of that in rubber) are small, $\ll 1$. So, usually, when a material behaves elastically, the strains are small and the linear approximation is consequently pretty good.

(ii) Continental drift can be measured on the surface of the earth using Very Long Baseline Interferometry, a technique in which two or more radio telescopes are used to detect interferometric fringes using radio waves from a distant point source. (A similar technique uses the Global Positioning System to achieve comparable accuracy.) By observing the fringes, it is possible to detect changes in the spacing between the telescopes as small as a fraction of a wavelength (~ 1 cm). As the telescopes are typically 1000km apart, this means that dimensionless strains $\sim 10^{-8}$ can be measured. Now, the continents drift apart on a timescale $\lesssim 10^8$yr., so it takes roughly a year for these changes to grow large enough to be measured. Such techniques are becoming useful for monitoring earthquake faults.

(iii) The smallest time-varying strains that have been measured so far involve laser interferometer gravitational wave detectors such as LIGO. In each arm of a LIGO interferometer, two mirrors hang freely, separated by 4 km. In 2005 their separations are monitored, at frequencies ~ 100 Hz, to $\sim 10^{-18}$ m, a thousandth the radius of a nucleon! The associated strain is 3×10^{-22}. Although these strains are not associated with an elastic solid, they do indicate the high accuracy of optical measurement techniques.

****

EXERCISES

Exercise 11.1 *Derivation and Practice: Reconstruction of a Tensor from its Irreducible Tensorial Parts.*
Using Eqs. (1), (2), and (3) of Box 11.2, show that $\frac{1}{3}\Theta g_{ij} + \Sigma_{ij} + R_{ij}$ is equal to S_{ij}.

Exercise 11.2 *Example: The Displacement Vectors Associated with Expansion, Rotation and Shear*

(a) Consider a strain that is pure expansion, $S_{ij} = \frac{1}{3}\Theta g_{ij}$. Using Eq. (11.4) show that, in the vicinity of a chosen point, the displacement vector is $\xi_i = \frac{1}{3}\Theta x_i$. Draw this displacement vector field.

(b) Similarly, draw $\boldsymbol{\xi}(\mathbf{x})$ for a strain that is pure rotation. [Hint: express $\boldsymbol{\xi}$ in terms of the vectorial angle $\boldsymbol{\phi}$ with the aid of Eq. (11.10a).]

(c) Draw $\boldsymbol{\xi}(\mathbf{x})$ for a strain that is pure shear. To simplify the drawing, assume that the shear is confined to the x-y plane, and make your drawing for a shear whose only nonzero components are $\Sigma_{xy} = \Sigma_{yx}$. Compare your drawing with Fig. 11.3, where the nonzero components are $\Sigma_{xx} = -\Sigma_{yy}$.

****

11.3 Stress and Elastic Moduli

11.3.1 Stress Tensor

The forces acting within an elastic solid are measured by a second rank tensor, the *stress tensor* introduced in Sec. 1.12.1 (which is also the spatial part of the stress-energy tensor of Sec. 1.12.2). Let us recall the definition of this stress tensor:

Consider two small, contiguous regions in a solid. If we take a small element of area $d\boldsymbol{\Sigma}$ in the contact surface with its positive sense[3] (same as direction of $d\boldsymbol{\Sigma}$ viewed as a vector) pointing from the first region toward the second, then the first region exerts a force $d\mathbf{F}$ (not necessarily normal to the surface) on the second through this area. The force the second region exerts on the first (through the area $-d\boldsymbol{\Sigma}$) will, by Newton's third law, be equal and opposite to that force. The force and the area of contact are both vectors and there is a linear relationship between them. (If we double the area, we double the force.) The two vectors therefore will be related by a second rank tensor, the stress tensor $\mathbf{T}$:

$$\boxed{d\mathbf{F} = \mathbf{T}\cdot d\boldsymbol{\Sigma} = \mathbf{T}(\ldots, d\boldsymbol{\Sigma})\ ; \quad \text{i.e., } dF_i = T_{ij}d\Sigma_j\ .} \tag{11.11}$$

[3]For a discussion of area elements including their positive sense, see Sec. 1.11.

Thus, the tensor $\mathbf{T}$ is the net (vectorial) force per unit (vectorial) area that a body exerts upon its surroundings. Be aware that many books on elasticity (e.g. Landau and Lifshitz 1986) define the stress tensor with the opposite sign to (11.11). Also be careful not to confuse the shear tensor Σ_{jk} with the vectorial infinitesimal surface area $d\Sigma_j$.

We often need to compute the total elastic force acting on some finite volume $\mathcal{V}$. Let us now make an important assumption, which we discuss in Sec. 11.3.4, namely that the stress is determined by local conditions and can be computed from the local arrangement of atoms. If this assumption is valid, then (as we shall see in Sec. 11.3.4), we can compute the total force acting on the volume element by integrating the stress over its surface $\partial\mathcal{V}$:

$$\mathbf{F} = -\int_{\partial\mathcal{V}} \mathbf{T}\cdot d\mathbf{\Sigma} = -\int_{\mathcal{V}} \boldsymbol{\nabla}\cdot\mathbf{T} dV \ , \tag{11.12}$$

where we have invoked Gauss' theorem, and the minus sign is because, for a closed surface $\partial\mathcal{V}$ (by convention), $d\mathbf{\Sigma}$ points out of $\mathcal{V}$ instead of into it.

Equation (11.12) must be true for arbitrary volumes and so we can identify the *elastic force density* $\mathbf{f}$ acting on an elastic solid as

$$\boxed{\mathbf{f} = -\boldsymbol{\nabla}\cdot\mathbf{T} \ .} \tag{11.13}$$

In elastostatic equilibrium, this force density must balance all other volume forces acting on the material, most commonly the gravitational force density so that

$$\boxed{\mathbf{f} + \rho\mathbf{g} = 0} \tag{11.14}$$

where $\mathbf{g}$ is the gravitational acceleration. (Again, there should be no confusion between the vector $\mathbf{g}$ and the metric tensor $\mathbf{g}$.) There are other possible external forces, some of which we shall encounter later in a fluid context, e.g. an electromagnetic force density. These can be added to Eq. (11.14).

Just as for the strain, the stress-tensor $\mathbf{T}$ can be decomposed into its irreducible tensorial parts, a pure trace (the *pressure* P) and a symmetric trace-free part (the shear stress):

$$\mathbf{T} = P\mathbf{g} + \mathbf{T}^{\rm shear} \ ; \quad P = \frac{1}{3}{\rm Tr}(\mathbf{T}) = \frac{1}{3}T_{ii} \ . \tag{11.15}$$

(There is no antisymmetric part because the stress tensor is symmetric, as we saw in Sec. 1.12.) Fluids at rest exert isotropic stresses, i.e. $\mathbf{T} = P\mathbf{g}$. They cannot exert shear stress when at rest, though when moving and shearing they can exert a viscous shear stress, as we shall discuss extensively in Part IV (especially Sec. 12.6).

In SI units, stress is measured in units of Pascals, denoted Pa

$$1{\rm Pa} = 1{\rm N/m}^2 = 1\frac{{\rm kg\,m/s}^2}{{\rm m}^2} \ , \tag{11.16}$$

or sometimes in GPa $= 10^9$ Pa. In cgs units, stress is measured in dyne/cm^2. Note that 1 Pa $= 10$ dyne/cm^2.

Now let us consider some examples of stresses:

(i) Atmospheric pressure is equal to the weight of the air in a column of unit area extending above the earth, and thus is roughly $P \sim \rho g H \sim 10^5$Pa, where $\rho \simeq 1$ kg m^{-3} is the density of air, $g \simeq 10$m s^{-2} is the acceleration of gravity at the earth's surface, and $H \simeq 10$km is the atmospheric scale height. Thus 1 atmosphere is $\sim 10^5$ Pa (or, more precisely, 1.01325×10^5 Pa). The stress tensor is isotropic.

(ii) Suppose we hammer a nail into a block of wood. The hammer might weigh $m \sim 0.3$kg and be brought to rest from a speed of $v \sim 10$m s^{-1} in a distance of, say, $d \sim 3$mm. Then the average force exerted on the wood by the nail is $F \sim mv^2/d \sim 10^4$N. If this is applied over an effective area $A \sim 1$mm^2, then the magnitude of the typical stress in the wood is $\sim F/A \sim 10^{10}$Pa $\sim 10^5$atmosphere. There is a large shear component to the stress tensor, which is responsible for separating the fibers in the wood as the nail is hammered.

(iii) Neutron stars are as massive as the sun, $M \sim 2 \times 10^{30}$ kg, but have far smaller radii, $R \sim 10$km. Their surface gravities are therefore $g \sim GM/R^2 \sim 10^{12}$m s^{-2}, a billion times that encountered on earth. They have solid crusts of density $\rho \sim 10^{17}$kg m^{-3} that are about 1km thick. The magnitude of the stress at the base of a neutron-star crust will then be $P \sim \rho g H \sim 10^{31}$Pa! This stress will be mainly hydrostatic, though as the material is solid, a modest portion will be in the form of a shear stress.

(iv) As we shall discuss in Chap. 27, a popular cosmological theory called *inflation* postulates that the universe underwent a period of rapid, exponential expansion during its earliest epochs. This expansion was driven by the stress associated with a *false vacuum*. The action of this stress on the universe can be described quite adequately using a classical stress tensor. If the interaction energy is $E \sim 10^{15}$GeV, the supposed scale of grand unification, and the associated length scale is the Compton wavelength associated with that energy $l \sim \hbar c/E$, then the magnitude of the stress is $\sim E/l^3 \sim 10^{97}(E/10^{15}\text{GeV})^4$ Pa.

(v) Elementary particles interact through forces. Although it makes no sense to describe this interaction using classical elasticity, it does make sense to make order of magnitude estimates of the associated stress. One promising model of these interactions involves *fundamental strings* with mass per unit length $\mu = g_s^2 c^2/8\pi G \sim 0.1$ Megaton/Fermi (where Megaton is not the TNT equivalent!), and cross section of order the Planck length squared, ${L_P}^2 = \hbar G/c^3 \sim 10^{-70}$ m^2, and tension (negative pressure) $T_{zz} \sim \mu c^2/{L_P}^2 \sim 10^{110}$ Pa. Here $\hbar$, G and c are Planck's (reduced) constant, Newton's gravitation constant, and the speed of light, and $g_s^2 \sim 0.025$ is the string coupling constant.

(vi) The highest possible stress is presumably found associated with singularities, for example at the creation of the universe or inside a black hole. Here the characteristic energy is the Planck energy $E_P = (\hbar c^5/G)^{1/2} \sim 10^{19}$ GeV, the lengthscale is the Planck length $L_P = (\hbar G/c^3)^{1/2} \sim 10^{-35}$ m, and the associated ultimate stress is $\sim 10^{114}$ Pa.

11.3.2 Elastic Moduli and Elastostatic Stress Balance

Having introduced the stress and the strain tensors, we are now in a position to generalize Hooke's law by postulating a linear relationship between them. The most general linear equation relating two second rank tensors will involve a fourth rank tensor known as the *elastic modulus tensor*, $\mathbf{Y}$. In slot-naming index notation,

$$T_{ij} = -Y_{ijkl}S_{kl} \tag{11.17}$$

Now, a general fourth rank tensor in three dimensions has $3^4 = 81$ independent components. Elasticity can get complicated! However, the situation need not be so dire. There are several symmetries that we can exploit. Let us look first at the general case. As the stress tensor is symmetric, and only the symmetric part of the strain tensor creates stress (i.e., a solid-body rotation through some vectorial angle $\boldsymbol{\phi}$ produces no stress), $\mathbf{Y}$ is symmetric in its first pair of slots and also in its second pair: $Y_{ijkl} = Y_{jikl} = Y_{ijlk}$. There are therefore 6 independent components Y_{ijkl} for variable i, j and fixed k, l, and *vice versa*. In addition, as we show below, $\mathbf{Y}$ is symmetric under an interchange of its first and second pairs of slots: $Y_{ijkl} = Y_{klij}$. There are therefore $(6 \times 7)/2 = 21$ independent components in $\mathbf{Y}$. This is an improvement over 81. Many substances, notably crystals, exhibit additional symmetries and this can reduce the number of independent components considerably.

The simplest, and in fact most common, case arises when the medium is *isotropic*. In other words, there are no preferred directions in the material. This occurs when the solid is polycrystalline or amorphous and completely disordered on a scale large compared with the atomic spacing, but small compared with the solid's inhomogeneity scale.

If a body is isotropic, then its elastic properties must be describable by scalars. Now, the stress tensor $\mathbf{T}$, being symmetric, must have just two irreducible tensorial parts, $\mathbf{T}$ =(a scalar P)$\mathbf{g}$+(a trace-free symmetric part $\mathbf{T}^{\rm shear}$); and the parts of the strain that can produce this $\{P, \mathbf{T}^{\rm shear}\}$ are the scalar expansion Θ and the trace-free, symmetric shear $\boldsymbol{\Sigma}$, but not the rotation. The only linear, coordinate-independent relationship between these $\{P, \mathbf{T}^{\rm shear}\}$ and $\{\Theta, \boldsymbol{\Sigma}\}$ involving solely scalars is $P = -K\Theta$, $T^{\rm shear} = -2\mu\boldsymbol{\Sigma}$, corresponding to a total stress tensor

$$\boxed{\mathbf{T} = -K\Theta\mathbf{g} - 2\mu\boldsymbol{\Sigma}\ .} \tag{11.18}$$

Here K is called the *bulk modulus* and μ the *shear modulus*, and the factor 2 is included for purely historical reasons. In Sec. 11.4 we will deduce the relationship of these elastic moduli to Young's modulus E (which appears in Hooke's law for the stress in a stretched rod or fiber [Eq. (11.1) and Fig. 11.1]). In some treatments and applications of elasticity, μ is called the *first Lame coefficient*, and a *second Lame coefficient* $\lambda \equiv K - \frac{2}{3}\mu$ is introduced and used in place of K.

It is commonly the case that the elastic moduli K and μ are constant, i.e. are independent of location in the medium, even though the medium is stressed in an inhomogeneous way. (This is because the strains are small and thus perturb the material properties by only small amounts.) If so, we can deduce (Ex. 11.3) an expression for the elastic force density inside the body [Eq. (11.13)]:

$$\boxed{\mathbf{f} = -\boldsymbol{\nabla}\cdot\mathbf{T} = K\boldsymbol{\nabla}\Theta + 2\mu\boldsymbol{\nabla}\cdot\boldsymbol{\Sigma} = \left(K + \frac{1}{3}\mu\right)\boldsymbol{\nabla}(\boldsymbol{\nabla}\cdot\boldsymbol{\xi}) + \mu\nabla^2\boldsymbol{\xi}\ .} \tag{11.19}$$

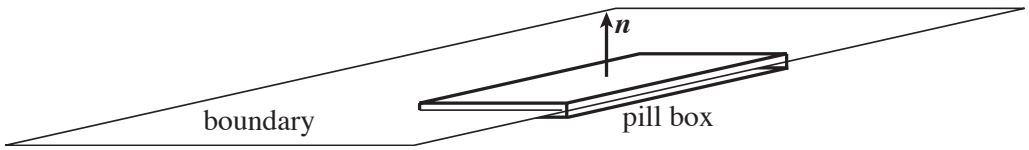

Fig. 11.4: Pill box used to derive boundary conditions in electrostatics and elastostatics.

Here $\boldsymbol{\nabla}\cdot\boldsymbol{\Sigma}$ in index notation is $\Sigma_{ij;j}=\Sigma_{ji;j}$. Extra terms must be added if we are dealing with less symmetric materials. However, in this book Eq. (11.19) will be sufficient for our needs.

If no other countervailing forces act in the interior of the material (e.g., if there is no gravitational force), and if, as in this chapter, the material is in a static, equilibrium state rather than vibrating dynamically, then this force density will have to vanish throughout the material's interior. This vanishing of $\mathbf{f}\equiv-\boldsymbol{\nabla}\cdot\mathbf{T}$ is just a fancy version of Newton's law for static situations, $\mathbf{F}=m\mathbf{a}=0$. If the material has density ρ and is pulled on by a gravitational acceleration $\mathbf{g}$, then the sum of the elastostatic force per unit volume and gravitational force per unit volume must vanish, $\mathbf{f}+\rho\mathbf{g}=0$.

When external forces are applied to the surface of an elastic body (for example, when one pushes on the face of a cylinder) and gravity acts on the interior, the distribution of the strain $\boldsymbol{\xi}(\mathbf{x})$ inside the body can be computed by solving the zero-internal-force equation

$$\boxed{\mathbf{f}+\rho\mathbf{g}=\left(K+\frac{1}{3}\mu\right)\boldsymbol{\nabla}(\boldsymbol{\nabla}\cdot\boldsymbol{\xi})+\mu\nabla^2\boldsymbol{\xi}+\rho\mathbf{g}=0} \tag{11.20}$$

subject to boundary conditions provided by the applied forces.

Solving this equation for $\boldsymbol{\xi}(\mathbf{x})$, subject to specified boundary conditions, is a problem in *elastostatics* analogous to solving Maxwell's equations for an electric field subject to boundary conditions in *electrostatics*, or for a magnetic field subject to boundary conditions in *magnetostatics*, and the types of solution techniques used in electrostatics and magnetostatics can also be used here — e.g. separation of variables and Green's functions. We shall explore examples in Sec. 11.6.2 and Exs. 11.14 and 11.15 below.

In electrostatics one can derive boundary conditions by integrating Maxwell's equations over the interior of a thin box (a "pill box") with parallel faces that snuggle up to the boundary (Fig. 11.4). For example, by integrating $\boldsymbol{\nabla}\cdot\mathbf{E}=\rho_e/\epsilon_o$ over the interior of the pill box, then applying Gauss's law to convert the left side to a surface integral, we obtain the junction condition that the discontinuity in the normal component of the electric field is equal $1/\epsilon_o$ times the surface charge density. Similarly, in elastostatics one can derive boundary conditions by integrating the elastostatic equation $\boldsymbol{\nabla}\cdot\mathbf{T}=0$ over the pill box of Fig. 11.4 and then applying Gauss's law:

$$0=\int_{\mathcal{V}}\boldsymbol{\nabla}\cdot\mathbf{T}dV=\int_{\partial\mathcal{V}}\mathbf{T}\cdot d\boldsymbol{\Sigma}=\int_{\partial\mathcal{V}}\mathbf{T}\cdot\mathbf{n}dA=[(\mathbf{T}\cdot\mathbf{n})_{\text{upper face}}-(\mathbf{T}\cdot\mathbf{n})_{\text{lower face}}]A\ . \tag{11.21}$$

Here in the next-to-last expression we have used $d\boldsymbol{\Sigma}=\mathbf{n}dA$ where dA is the scalar area element and $\mathbf{n}$ is the unit normal to the pill-box face, and in the last term we have assumed

the pill box has a small face so $\mathbf{T}\cdot\mathbf{n}$ can be treated as constant and be pulled outside the integral. The result is the boundary condition that $\mathbf{T}\cdot\mathbf{n}$ *must be continuous across any boundary*, i.e. in index notation, $T_{ij}n_j$ is continuous.

Physically this is nothing but the law of force balance across the boundary: *The force per unit area acting from the lower side to the upper side must be equal and opposite to that acting from upper to lower.* As an example, if the upper face is bounded by vacuum then the solid's stress tensor must satisfy $T_{ij}n_j = 0$ at the surface. If a normal pressure P is applied by some external agent at the upper face, then the solid must respond with a normal force equal to P: $n_iT_{ij}n_j = P$. If a vectorial force per unit area $\mathcal{F}_i$ is applied at the upper face by some external agent, then it must be balanced: $T_{ij}n_j = \mathcal{F}_i$.

11.3.3 Energy of Deformation

Take a wire of length ℓ and cross sectional area A, and stretch it (e.g. via the "Hooke's-law experiment" of Fig. 11.1) by an amount ζ' that grows gradually from 0 to $\Delta\ell$. When the stretch is ζ', the force that does the stretching is $F' = EA(\zeta'/\ell) = EV/\ell^2)\zeta'$; here $V = EA\ell$ is the wire's volume and E is its Young's modulus. As the wire is gradually lengthened, the stretching force F' does work

$$\begin{aligned} W &= \int_0^{\Delta\ell} F' d\zeta' = \int_0^{\Delta\ell} (EV/\ell)\zeta' d\zeta' \\ &= \frac{1}{2}EV(\Delta\ell/\ell)^2 \ . \end{aligned} \tag{11.22}$$

This tells us that the stored elastic energy per unit volume is

$$U = \frac{1}{2}E(\Delta\ell/\ell)^2 \tag{11.23}$$

To generalize this formula to three dimensions, consider an arbitrary but very small region $\mathcal{V}$ inside a body that has already been stressed by a displacement vector field ξ_i and is thus already experiencing an elastic stress T_{ij} given by the three-dimensional stress-strain relation (11.18). Imagine building up this displacement gradually from zero at the same rate everywhere in and around $\mathcal{V}$, so at some moment during the buildup the displacement field is $\xi_i' = \xi_i\epsilon$ (with the parameter ϵ gradually growing from 0 to 1). At that moment, the stress tensor (by virtue of the linearity of the stress-strain relation) is $T_{ij}' = T_{ij}\epsilon$. On the boundary $\partial\mathcal{V}$ of the region $\mathcal{V}$, this stress exerts a force $\Delta F_i' = -T_{ij}'\Delta\Sigma_j$ across any surface element $\Delta\Sigma_j$, from the exterior of ∂V to its interior. As the displacement grows, this surface force does the following amount of work on $\mathcal{V}$:

$$\Delta W_{\rm surf} = \int \Delta F_i' d\xi_i' = \int (-T_{ij}'\Delta\Sigma_j) d\xi_i' = -\int_0^1 T_{ij}\epsilon\Delta\Sigma_j\xi_i' d\epsilon = -\frac{1}{2}T_{ij}\Delta\Sigma_j\xi_i \ . \tag{11.24}$$

The total amount of work done can be computed by adding up the contributions from all the surface elements of $\partial\mathcal{V}$:

$$W_{\rm surf} = -\frac{1}{2}\int_{\partial\mathcal{V}} T_{ij}\xi_i d\Sigma_j = -\frac{1}{2}\int_{\mathcal{V}} (T_{ij}\xi_i)_{;j} dV \ = -\frac{1}{2}(T_{ij}\xi_i)_{;j}V \ . \tag{11.25}$$

In the second step we have used Gauss's theorem, and in the third step we have used the smallness of the region $\mathcal{V}$ to infer that the integrand is very nearly constant and the integral is the integrand times the total volume V of $\mathcal{V}$.

Does this equal the elastic energy stored in $\mathcal{V}$? The answer is "no", because we must also take account of the work done in the interior of $\mathcal{V}$ by gravity or any other non-elastic force that may be acting. Now, although it is not easy in practice to turn gravity off and then on, we must do so in this thought experiment: In the volume's final deformed state, the divergence of its elastic stress tensor is equal to the gravitational force density, $\boldsymbol{\nabla}\cdot\mathbf{T}=\rho\mathbf{g}$ [Eqs. (11.13) and (11.14]; and in the initial, undeformed and unstressed state, $\boldsymbol{\nabla}\cdot\mathbf{T}$ must be zero, whence so must be $\mathbf{g}$. Therefore, we must imagine growing the gravitational force proportional to ϵ just like we grow the displacement, strain and stress. During this growth, the gravitational force $\rho\mathbf{g}'V=\rho\mathbf{g}V\epsilon$ does the following amount of work on our tiny region $\mathcal{V}$:

$$W_{\rm grav}=\int\rho V\mathbf{g}'\cdot d\boldsymbol{\xi}'=\int_0^1\rho V\mathbf{g}\epsilon\cdot\boldsymbol{\xi}d\epsilon=\frac{1}{2}\rho V\mathbf{g}\cdot\boldsymbol{\xi}=\frac{1}{2}(\boldsymbol{\nabla}\cdot\mathbf{T})\cdot\boldsymbol{\xi}V=\frac{1}{2}T_{ij;j}\xi_iV\ . \quad (11.26)$$

The total work done to deform $\mathcal{V}$ is the sum of the work done by the elastic force (11.25) on its surface and the gravitational force (11.26) in its interior, $W_{\rm surf}+W_{\rm grav}=-\frac{1}{2}(\xi_iT_{ij})_{;j}V+\frac{1}{2}T_{ij;j}\xi_iV=-\frac{1}{2}T_{ij}\xi_{i;j}V$. This work gets stored in $\mathcal{V}$ as elastic energy, so the energy density is $U=-\frac{1}{2}T_{ij}\xi_{i;j}$. Inserting $T_{ij}=-K\Theta g_{ij}-2\mu\Sigma_{ij}$ and $\xi_{i;j}=\frac{1}{3}\Theta g_{ij}+\Sigma_{ij}+R_{ij}$ and performing some simple algebra that relies on the symmetry properties of the expansion, shear, and rotation (Ex. 11.5), we obtain

$$\boxed{U=\frac{1}{2}K\Theta^2+\mu\Sigma_{ij}\Sigma_{ij}\ .} \quad (11.27)$$

Note that this elastic energy density is always positive if the elastic moduli are positive — as they must be in order that matter be be stable to small perturbations.

For the more general, anisotropic case, expression (11.27) becomes [by virtue of the stress-strain relation $T_{ij}=-Y_{ijkl}\xi_{k;l}$, Eq. (11.17)]

$$U=\frac{1}{2}\xi_{i;j}Y_{ijkl}\xi_{k;l}\ . \quad (11.28)$$

The volume integral of the elastic energy density (11.27) or (11.28) can be used as an action from which to compute the stress, by varying the displacement (Ex. 11.6). Since only the part of $\mathbf{Y}$ that is symmetric under interchange of the first and second pairs of slots contributes to U, only that part can affect the action-principle-derived stress. Therefore, it must be that $Y_{ijkl}=Y_{klij}$. This is the symmetry we asserted earlier.

11.3.4 Molecular Origin of Elastic Stress

It is important to understand the microscopic origin of the elastic stress. Consider an ionic solid in which singly ionized ions (e.g. sodium and chlorine) attract their nearest neighbours through their mutual Coulomb attraction and repel their next nearest neighbors and so on.

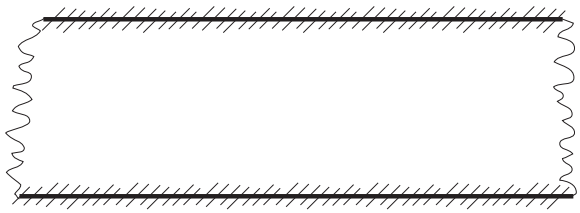

Fig. 11.5: Action of electromagnetic forces within a solid. If we compute the force acting on one side of a slice of material, the integral is dominated by interactions between atoms lying in the shaded area. The force is effectively a surface force rather than a volume force. In elastostatic equilibrium, the forces acting on the two sides of the slice are effectively equal and opposite.

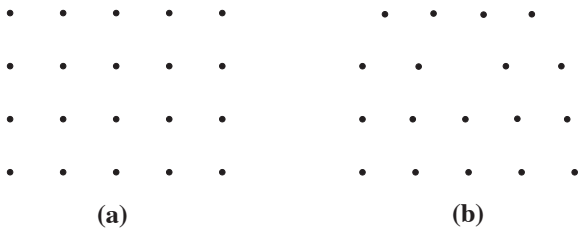

Fig. 11.6: a) A perfect crystal in which the atoms are organized in a perfectly repeating lattice can develop very large shear strains without yielding. b) Real materials contain dislocations which greatly reduce their rigidity. The simplest type of dislocation, shown here, is the *edge dislocation*. The dislocation will move and the crystal will undergo inelastic deformation when the stress is typically less than one per cent of the yield shear stress for a perfect crystal.

Overall, there is a net attraction, which is balanced by the short range repulsion of the bound electrons. Now consider a thin slice of material of thickness intermediate between the interatomic spacing and the solid's inhomogeneity scale, a few atomic spacings thick (Figure 11.5). If we calculate the force acting on the material in the slice, exerted by external atoms on one side of the slice, we find that the sum converges very close to the boundary. Although the electrostatic force between individual atoms is long range, the material is electrically neutral and, when averaged over many atoms, the net electric force is of short range. We can therefore treat the net force acting on a region that is large enough to encompass many atoms, but much smaller than the body's inhomogeneity scale, as a surface force governed by local conditions in the material. This is essential if we are to be able to write down a local, linear stress-strain relation $T_{ij} = -Y_{ijkl}S_{kl}$. This need not have been the case and there are circumstances when a long range force develops. One example occurs with certain types of crystal (e.g. tourmaline) which develop internal, *piezoelectric* fields when strained.

Our treatment so far has implicitly made the assumption that matter is continuous on all scales and that derivatives are mathematically well-defined. Of course, this is not the case. In fact, we not only need to acknowledge the existence of atoms, we must use this fact to compute the elastic moduli.

We can estimate the elastic moduli in ionic or metallic materials by observing that, if a crystal lattice were to be given a dimensionless strain of order unity, then the elastic stress would be of order the electrostatic force between adjacent ions divided by the area

Substance	K	μ	E	ν	c_L	c_T
	GPa	GPa	GPa		km s^{-1}	km s^{-1}
Steel	170	81	210	0.29	5.9	3.2
Copper	130	45	120	0.34	4.6	2.2
Glass	47	28	70	0.25	5.8	3.3
Rubber	10	0.0007	0.002	0.50	1.0	0.03

Table 11.1: Bulk, Shear and Young's moduli and Poisson's ratio for a range of materials. The final two columns quote the longitudinal and transverse sound speeds defined in the following chapter.

associated with each ion. If the lattice spacing is $a \sim 2$Å and the ions are singly charged, then $K, \mu \sim e^2/4\pi\epsilon_0 a^4 \sim 100$ GPa. This is about a million atmospheres. Covalently bonded compounds are less tightly bound and have somewhat smaller elastic moduli. See Table 11.1.

It might be thought, on the basis of this argument, that crystals can be subjected to strains of order unity before they attain their elastic limits. However, as explained above, most materials are only elastic for strains $\lesssim 10^{-3}$. The reason for this difference is that crystals are generally imperfect and are laced with *dislocations*. Relatively small stresses suffice for the dislocations to move through the solid and for the crystal thereby to undergo permanent deformation (Fig. 11.6).

****

EXERCISES

Exercise 11.3 *Derivation and Practice: Elastic Force Density*
From Eq. (11.18) derive expression (11.19) for the elastostatic force density inside an elastic body.

Exercise 11.4 **** Practice: Biharmonic Equation*
A homogeneous, isotropic, elastic solid is in equilibrium under (uniform) gravity and applied surface stresses. Use Eq. (11.19) to show that the displacement inside it $\boldsymbol{\xi}(\mathbf{x})$ is biharmonic, i.e. it satisfies the differential equation

$$\boxed{\nabla^2\nabla^2\boldsymbol{\xi} = 0\ .} \tag{11.29a}$$

Show also that the expansion Θ satisfies the Lapace equation

$$\boxed{\nabla^2\Theta = 0\ .} \tag{11.29b}$$

Exercise 11.5 *Derivation and Practice: Elastic Energy*
Beginning with $U = -\frac{1}{2}T_{ij}\xi_{i;j}$ [text following Eq. (11.26)], derive $U = \frac{1}{2}K\Theta^2 + \mu\Sigma_{ij}\Sigma_{ij}$ for the elastic energy density inside a body.

Exercise 11.6 *Derivation and Practice: Action Principle for Elastic Stress*
For an anisotropic, elastic body with elastic energy density $U = \frac{1}{2}\xi_{i;j}Y_{ijkl}\xi_{k;l}$, integrate this energy density over a three-dimensional region $\mathcal{V}$ (not necessarily small) to get the total elastic energy $\mathcal{E}$. Now, consider a small variation $\delta\xi_i$ in the displacement field. Evaluate the resulting change $\delta\mathcal{E}$ in the elastic energy without using the relation $T_{ij} = -Y_{ijkl}\xi_{k;l}$. Convert to a surface integral over $\partial\mathcal{V}$ and therefrom infer the stress-strain relation $T_{ij} = -Y_{ijkl}\xi_{k;l}$.

Exercise 11.7 *Problem: Order of Magnitude Estimates*

(a) What length of steel wire can hang vertically without breaking?

(b) What is the maximum size of a non-spherical asteroid? [Hint: if the asteroid is too large, its gravity will deform it into a spherical shape.]

(c) Can a helium balloon lift the tank used to transport the helium?

****

11.4 Young's Modulus and Poisson's Ratio for an Isotropic Material: A Simple Elastostatics Problem

As a simple example of an elastostatics problem, we shall explore the connection between our three-dimensional theory of stress and strain, and the one-dimensional Hooke's law [Fig. 11.1 and Eq. (11.1)].

Consider a thin rod of square cross section hanging along the $\mathbf{e}_z$ direction of a Cartesian coordinate system (Fig. 11.1). Subject the rod to a stretching force applied normally and uniformly at its ends. (It could just as easily be a rod under compression.) Its sides are free to expand transversely, since no force acts on them, $dF_i = T_{ij}d\Sigma_j = 0$. As the rod is slender, vanishing of dF_i at its x and y sides implies to high accuracy that the stress components T_{ix} and T_{iy} will vanish throughout the interior; otherwise there would be a very large force density $T_{ij;j}$ inside the rod. Using $T_{ij} = -K\Theta g_{ij} - 2\mu\Sigma_{ij}$, we then obtain

$$T_{xx} = -K\Theta - 2\mu\Sigma_{xx} = 0 \ , \tag{11.30a}$$
$$T_{yy} = -K\Theta - 2\mu\Sigma_{yy} = 0 \ , \tag{11.30b}$$
$$T_{yz} = -2\mu\Sigma_{yz} = 0 \ , \tag{11.30c}$$
$$T_{xz} = -2\mu\Sigma_{xz} = 0 \ , \tag{11.30d}$$
$$T_{xy} = -2\mu\Sigma_{xy} = 0 \ , \tag{11.30e}$$
$$T_{zz} = -K\Theta - 2\mu\Sigma_{zz} \ . \tag{11.30f}$$

From the first two of these equations and $\Sigma_{xx} + \Sigma_{yy} + \Sigma_{zz} = 0$ we obtain a relationship between the expansion and the nonzero components of the shear,

$$K\Theta = \mu\Sigma_{zz} = -2\mu\Sigma_{xx} = -2\mu\Sigma_{yy} \ ; \tag{11.31}$$

and from this and Eq. (11.30f) we obtain $T_{zz} = -3K\Theta$. The decomposition of S_{ij} into its irreducible tensorial parts tells us that $S_{zz} = \xi_{z;z} = \Sigma_{zz} + \frac{1}{3}\Theta$, which becomes, upon using Eq. (11.31), $\xi_{z;z} = [(3K+\mu)/3\mu]\Theta$. Combining with $T_{zz} = -3K\Theta$ we obtain Hooke's law and an expression for Young's modulus E in terms of the bulk and shear moduli:

$$\frac{-T_{zz}}{\xi_{z;z}} = \frac{9\mu K}{3K+\mu} = E\ . \tag{11.32}$$

It is conventional to introduce *Poisson's ratio*, ν, which is defined to be minus the ratio of the lateral strain to the longitudinal strain during a deformation of this type, in which the transverse motion is unconstrained. It can be expressed as a ratio of elastic moduli as follows:

$$\nu = -\frac{\xi_{x,x}}{\xi_{z,z}} = -\frac{\Sigma_{xx} + \frac{1}{3}\Theta}{\Sigma_{zz} + \frac{1}{3}\Theta} = \frac{3K - 2\mu}{2(3K+\mu)}\ , \tag{11.33}$$

where we have used Eq. (11.31). We tabulate these and their inverses for future use:

$$\boxed{E = \frac{9\mu K}{3K+\mu}\ , \quad \nu = \frac{3K-2\mu}{2(3K+\mu)}\ ; \qquad K = \frac{E}{3(1-2\nu)}\ , \quad \mu = \frac{E}{2(1+\nu)}.} \tag{11.34}$$

We have already remarked that mechanical stability of a solid requires that $K, \mu > 0$. Using Eq. (11.34), we observe that this imposes a restriction on Poisson's ratio, namely that $-1 < \nu < 1/2$. For metals, Poisson's ratio is typically 1/3 and the shear modulus is roughly half the bulk modulus. For a substance that is easily sheared but not easily compressed, like rubber, the bulk modulus is relatively high and $\nu \simeq 1/2$ (cf. Table 11.1.) For some exotic materials, Poison's ratio can be negative (cf. Yeganeh-Haeri *et al* 1992).

Although we derived them for a square strut under compression, our expressions for Young's modulus and Poisson's ratio are quite general. To see this, observe that the derivation would be unaffected if we combined many parallel, square fibers together. All that is necessary is that the transverse motion be free so that the only applied force is normal to a pair of parallel faces.

11.5 T2 Cylindrical and Spherical Coordinates: Connection Coefficients and Components of Strain

Thus far, in our discussion of elasticisty, we have resticted ourselves to Cartesian coordinates. However, many problems in elasticity are most efficiently solved using cylindrical or spherical coordinates, so in this section we shall develop some mathematical tools for those coordinate systems. In doing so we follow the vectorial conventions of standard texts on electrodynamics and quantum mechanics (e.g., Jackson 1999, and Messiah 1962): We introduce an *orthonormal* set of basis vectors associated with each of our curvilinear coordinate systems; the coordinate lines are orthogonal to each other, and the basis vectors have unit lengths and point along the coordinate lines. In our study of continuum mechanics (Part III – Elasticity, Part IV – Fluid Mechanics, and Part V – Plasma Physics), we shall follow this

practice. Then in studying General Relativity and Cosmology (Part VI) we shall introduce and use basis vectors that are *not* orthonormal.

Our notation for cylindrical coordinates is (ϖ, ϕ, z); ϖ (pronounced "pomega") is distance from the z axis, and ϕ is angle around the z axis, so

$$\varpi = \sqrt{x^2 + y^2}\ , \quad \phi = \arctan(y/x)\ . \tag{11.35a}$$

The unit basis vectors that point along the coordinate axes are denoted $\mathbf{e}_\varpi$, $\mathbf{e}_\phi$, $\mathbf{e}_z$, and are related to the Cartesian basis vectors by

$$\mathbf{e}_\varpi = (x/\varpi)\mathbf{e}_x + (y/\varpi)\mathbf{e}_y\ , \quad \mathbf{e}_\phi = -(y/\varpi)\mathbf{e}_x + (x/\varpi)\mathbf{e}_y\ , \quad \mathbf{e}_z = \text{Cartesian } \mathbf{e}_z\ . \tag{11.35b}$$

Our notation for spherical coordinates is (r, θ, ϕ), with (as should be very familiar)

$$r = \sqrt{x^2 + y^2 + z^2}\ , \quad \theta = \arccos(z/r)\ , \quad \phi = \arctan(y/x)\ . \tag{11.36a}$$

The unit basis vectors associated with these coordinates are

$$\mathbf{e}_r = \frac{x}{r}\mathbf{e}_x + \frac{y}{r}\mathbf{e}_y + \frac{z}{r}\mathbf{e}_z\ , \quad \mathbf{e}_\theta = \frac{z}{r}\mathbf{e}_\varpi - \frac{\varpi}{r}\mathbf{e}_z\ , \quad \mathbf{e}_\phi = -\frac{y}{\varpi}\mathbf{e}_x + \frac{x}{\varpi}\mathbf{e}_y\ . \tag{11.36b}$$

Because our bases are orthonormal, the components of the metric of 3-dimensional space retain the Kronecker-delta values

$$\boxed{g_{jk} \equiv \mathbf{e}_j \cdot \mathbf{e}_k = \delta_{jk},} \tag{11.37}$$

which permits us to keep all vector and tensor indices down, by contrast with spacetime where we must distinguish between up and down; cf. Sec. 1.5.[4]

In Jackson (1999), Messiah (1962) and other standard texts, formulas are written down for the gradient and Laplacian of a scalar field, and the divergence and curl of a vector field, in cylindrical and spherical coordinates; and one uses these formulas over and over again. In elasticity theory we deal largely with second rank tensors, and will need formulae for their various derivatives in cylindrical and spherical coordinates. In this book we introduce a mathematical tool, *connection coefficients* Γ_{ijk}, by which those formulae can be derived when needed.

The connection coefficients quantify the turning of the orthonormal basis vectors as one moves from point to point in Euclidean 3-space; i.e., they tell us how the basis vectors at one point in space are *connected to* (related to) those at another point. More specifically, we define Γ_{ijk} by the two equivalent relations

$$\boxed{\nabla_k \mathbf{e}_j = \Gamma_{ijk}\mathbf{e}_i\ ; \quad \Gamma_{ijk} = \mathbf{e}_i \cdot (\nabla_k \mathbf{e}_j)\ ;} \tag{11.38}$$

here $\nabla_k \equiv \nabla_{\mathbf{e}_k}$ is the directional derivative along the orthonormal basis vector $\mathbf{e}_k$; cf. Eq. (1.54a). Notice that (as is true quite generally; cf. Sec. 1.9) the differentiation index comes

[4] Occasionally, e.g. in the useful equation $\epsilon_{ijm}\epsilon_{klm} = \delta^{ij}_{kl} \equiv \delta^i_k\delta^j_l - \delta^i_l\delta^j_k$ [Eq. (1.61)], it is convenient to put some indices up; but because $g_{jk} = \delta_{jk}$, any component with an index up is equal to that same component with an index down; e.g., $\delta^i_k \equiv \delta_{ik}$.

last on Γ. Because our basis is orthonormal, it must be that $\nabla_k(\mathbf{e}_i \cdot \mathbf{e}_j) = 0$. Expanding this out using the standard rule for differentiating products, we obtain $\mathbf{e}_j \cdot (\nabla_k \mathbf{e}_i) + \mathbf{e}_i \cdot (\nabla_k \mathbf{e}_j) = 0$. Then invoking the definition (11.38) of the connection coefficients, we see that Γ_{ijk} is antisymmetric on its first two indices:

$$\boxed{\Gamma_{ijk} = -\Gamma_{jik} \ .} \tag{11.39}$$

In Part VI, when we use non-orthonormal bases, this antisymmetry will break down.

It is straightforward to compute the connection coefficients for cylindrical and spherical coordinates from the definition (11.38), expressions (11.35b) and (11.36b) for the cylindrical and spherical basis vectors in terms of the Cartesian basis vectors, and from the fact that *in Cartesian coordinates the connection coefficients vanish* ($\mathbf{e}_x$, $\mathbf{e}_y$ and $\mathbf{e}_z$ do not rotate as one moves through Euclidean 3-space). One can also deduce the cylindrical and spherical connection coefficients by drawing pictures of the basis vectors and observing how they change from point to point. For cylindrical coordinates, we see from Fig. 11.7 that $\nabla_\phi \mathbf{e}_\varpi = \mathbf{e}_\phi/\varpi$. A similar pictorial calculation (which the reader is encouraged to do) reveals that $\nabla_\phi \mathbf{e}_\phi = -\mathbf{e}_\varpi/\varpi$. All other derivatives vanish. Therefore, *the only nonzero connection coefficients in cylindrical coordinates are*

$$\boxed{\Gamma_{\varpi\phi\phi} = -\frac{1}{\varpi}, \quad \Gamma_{\phi\varpi\phi} = \frac{1}{\varpi} \ ,} \tag{11.40}$$

which have the required antisymmetry [Eq. (11.39)]. Likewise, for spherical coordinates (Ex. 11.9)

$$\boxed{\Gamma_{\theta r\theta} = \Gamma_{\phi r\phi} = -\Gamma_{r\theta\theta} = -\Gamma_{r\phi\phi} = \frac{1}{r}, \quad \Gamma_{\phi\theta\phi} = -\Gamma_{\theta\phi\phi} = \frac{\cot\theta}{r} \ ;} \tag{11.41}$$

The connection coefficients are the keys to differentiating vectors and tensors. Consider the strain tensor $\mathbf{S} = \boldsymbol{\nabla\xi}$. Applying the product rule for differentiation, we obtain

$$\nabla_k(\xi_j \mathbf{e}_j) = (\nabla_k \xi_j)\mathbf{e}_j + \xi_j(\nabla_k \mathbf{e}_j) = \xi_{j,k}\mathbf{e}_j + \xi_j \Gamma_{ljk}\mathbf{e}_l \ . \tag{11.42}$$

Here the comma denotes the directional derivative, along a basis vector, of the components treated as scalar fields. For example, *in cylindrical coordinates* we have

$$\xi_{i,\varpi} = \frac{\partial \xi_i}{\partial \varpi} \ , \quad \xi_{i,\phi} = \frac{1}{\varpi}\frac{\partial \xi_i}{\partial \phi} \ , \quad \xi_{i,z} = \frac{\partial \xi_i}{\partial z} \ ; \tag{11.43}$$

and *in spherical coordinates* we have

$$\xi_{i,r} = \frac{\partial \xi_i}{\partial r} \ , \quad \xi_{i,\theta} = \frac{1}{r}\frac{\partial \xi_i}{\partial \theta} \ , \quad \xi_{i,\phi} = \frac{1}{r\sin\theta}\frac{\partial \xi_i}{\partial \phi} \ . \tag{11.44}$$

Taking the i'th component of Eq. (11.42) we obtain

$$\boxed{S_{ik} = \xi_{i;k} = \xi_{i,k} + \Gamma_{ijk}\xi_j \ .} \tag{11.45}$$

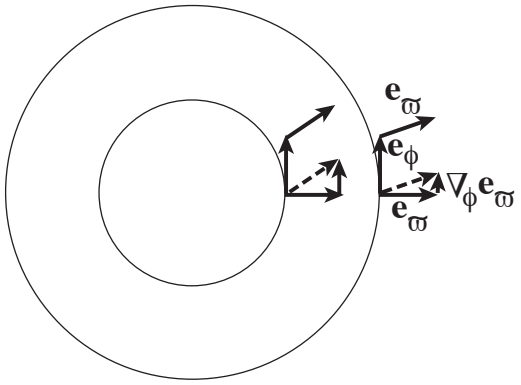

Fig. 11.7: Pictorial evaluation of $\Gamma_{\phi\varpi\phi}$. In the right-most assemblage of vectors we compute $\nabla_\phi \mathbf{e}_\varpi$ as follows: We draw the vector to be differentiated, $\mathbf{e}_\varpi$, at the tail of $\mathbf{e}_\phi$ (the vector along which we differentiate) and also at its head. We then subtract $\mathbf{e}_\varpi$ at the head from that at the tail; this difference is $\nabla_\phi \mathbf{e}_\varpi$. It obviously points in the $\mathbf{e}_\phi$ direction. When we perform the same calculation at a radius ϖ that is smaller by a factor 2 (left assemblage of vectors), we obtain a result, $\nabla_\phi \mathbf{e}_\varpi$, that is twice as large. Therefore the length of this vector must scale as $1/\varpi$. By looking quantitatively at the length at some chosen radius ϖ, one can see that the multiplicative coefficient is unity: $\nabla_\phi \mathbf{e}_\varpi = \frac{1}{\varpi}\mathbf{e}_\phi$. Comparing with Eq. (11.38), we deduce that $\Gamma_{\phi\varpi\phi} = 1/\varpi$.

Here $\xi_{i;k}$ are the nine components of the gradient of the vector field $\boldsymbol{\xi}(\mathbf{x})$ evaluated in any orthonormal basis. We can use Eq. (11.45) to evaluate the expansion $\Theta = \mathrm{Tr}\mathbf{S} = \boldsymbol{\nabla}\cdot\boldsymbol{\xi}$. Using Eq. (11.40) , (11.41) , we obtain

$$\begin{aligned}\Theta = \boldsymbol{\nabla}\cdot\boldsymbol{\xi} &= \frac{\partial \xi_\varpi}{\partial \varpi} + \frac{1}{\varpi}\frac{\partial \xi_\phi}{\partial \phi} + \frac{\partial \xi_z}{\partial z} + \frac{\xi_\varpi}{\varpi} \\ &= \frac{1}{\varpi}\frac{\partial}{\partial \varpi}(\varpi \xi_\varpi) + \frac{1}{\varpi}\frac{\partial \xi_\phi}{\partial \phi} + \frac{\partial \xi_z}{\partial z} \end{aligned} \tag{11.46}$$

in cylindrical coordinates, and

$$\begin{aligned}\Theta = \boldsymbol{\nabla}\cdot\boldsymbol{\xi} &= \frac{\partial \xi_r}{\partial r} + \frac{1}{r}\frac{\partial \xi_\theta}{\partial \theta} + \frac{1}{r\sin\theta}\frac{\partial \xi_\phi}{\partial \phi} + \frac{2\xi_r}{r} + \frac{\cot\theta \xi_\theta}{r} \\ &= \frac{1}{r^2}\frac{\partial}{\partial r}(r^2\xi_r) + \frac{1}{r\sin\theta}\frac{\partial}{\partial \theta}(\sin\theta\xi_\theta) + \frac{1}{r\sin\theta}\frac{\partial \xi_\phi}{\partial \phi} \end{aligned} \tag{11.47}$$

in spherical coordinates, in agreement with formulae in standard textbooks such as the flyleaf of Jackson (1999).

The components of the rotation are most easily deduced using $R_{ij} = -\epsilon_{ijk}\phi_k$ with $\boldsymbol{\phi} = \frac{1}{2}\boldsymbol{\nabla}\times\boldsymbol{\xi}$, and the standard expressions for the curl in cylindrical and spherical coordinates (e.g., Jackson 1999). Since the rotation does not enter into elasticity theory in a significant way, we shall refrain from writing down the results. The components of the shear are computed in Box 11.3.

By a computation analogous to Eq. (11.42) we can construct an expression for the gradient of a tensor of any rank. For a second rank tensor $\mathbf{T} = T_{ij}\mathbf{e}_i \otimes \mathbf{e}_j$ we obtain (Ex. 11.8)

$$\boxed{T_{ij;k} = T_{ij,k} + \Gamma_{ilk}T_{lj} + \Gamma_{jlk}T_{il}\ .} \tag{11.48}$$

Box 11.3
Shear Tensor in Spherical and Cylindrical Coordinates

Using our rules for forming the gradient of a vector we can derive a general expression for the shear tensor

$$\begin{aligned}\Sigma_{ij} &= \frac{1}{2}(\xi_{i;j}+\xi_{j;i}) - \frac{1}{3}\delta_{ij}\xi_{k;k} \\ &= \frac{1}{2}(\xi_{i,j}+\xi_{j,i}+\Gamma_{ilj}\xi_l+\Gamma_{jli}\xi_l) - \frac{1}{3}\delta_{ij}(\xi_{k,k}+\Gamma_{klk}\xi_l)\ . \end{aligned} \tag{1}$$

Evaluating this *in cylindrical coordinates* using the connection coefficients (11.40), we obtain

$$\begin{aligned}\Sigma_{\varpi\varpi} &= \frac{2}{3}\frac{\partial\xi_\varpi}{\partial\varpi} - \frac{1}{3}\frac{\xi_\varpi}{\varpi} - \frac{1}{3\varpi}\frac{\partial\xi_\phi}{\partial\phi} - \frac{1}{3}\frac{\partial\xi_z}{\partial z} \\ \Sigma_{\phi\phi} &= \frac{2}{3\varpi}\frac{\partial\xi_\phi}{\partial\phi} + \frac{2}{3}\frac{\xi_\varpi}{\varpi} - \frac{1}{3}\frac{\partial\xi_\varpi}{\partial\varpi} - \frac{1}{3}\frac{\partial\xi_z}{\partial z} \\ \Sigma_{zz} &= \frac{2}{3}\frac{\partial\xi_z}{\partial z} - \frac{1}{3}\frac{\partial\xi_\varpi}{\partial\varpi} - \frac{1}{3}\frac{\xi_\varpi}{\varpi} - \frac{1}{3\varpi}\frac{\partial\xi_\phi}{\partial\phi} \\ \Sigma_{\phi z} &= \Sigma_{z\phi} = \frac{1}{2\varpi}\frac{\partial\xi_z}{\partial\phi} + \frac{1}{2}\frac{\partial\xi_\phi}{\partial z} \\ \Sigma_{z\varpi} &= \Sigma_{\varpi z} = \frac{1}{2}\frac{\partial\xi_\varpi}{\partial z} + \frac{1}{2}\frac{\partial\xi_z}{\partial\varpi} \\ \Sigma_{\varpi\phi} &= \Sigma_{\phi\varpi} = \frac{1}{2}\frac{\partial\xi_\phi}{\partial\varpi} - \frac{\xi_\phi}{2\varpi} + \frac{1}{2\varpi}\frac{\partial\xi_\varpi}{\partial\phi}\ . \end{aligned} \tag{2}$$

Likewise, *in spherical coordinates* using the connection coefficients (11.41), we obtain

$$\begin{aligned}\Sigma_{rr} &= \frac{2}{3}\frac{\partial\xi_r}{\partial r} - \frac{2}{3r}\xi_r - \frac{\cot\theta}{3r}\xi_\theta - \frac{1}{3r}\frac{\partial\xi_\theta}{\partial\theta} - \frac{1}{3r\sin\theta}\frac{\partial\xi\phi}{\partial\phi} \\ \Sigma_{\theta\theta} &= \frac{2}{3r}\frac{\partial\xi_\theta}{\partial\phi} + \frac{\xi_r}{3r} - \frac{1}{3}\frac{\partial\xi_r}{\partial r} - \frac{\cot\theta\xi_\theta}{3r} - \frac{1}{3r\sin\theta}\frac{\partial\xi_\phi}{\partial\phi} \\ \Sigma_{\phi\phi} &= \frac{2}{3r\sin\theta}\frac{\partial\xi_\phi}{\partial\phi} + \frac{2\cot\theta\xi_\theta}{3r} + \frac{\xi_r}{3r} - \frac{1}{3}\frac{\partial\xi_r}{\partial r} - \frac{1}{3r}\frac{\partial\xi_\theta}{\partial\theta} \\ \Sigma_{\theta\phi} &= \Sigma_{\phi\theta} = \frac{1}{2r}\frac{\partial\xi_\phi}{\partial\theta} - \frac{\cot\theta\xi_\phi}{2r} + \frac{1}{2r\sin\theta}\frac{\partial\xi_\theta}{\partial\phi} \\ \Sigma_{\phi r} &= \Sigma_{r\phi} = \frac{1}{2r\sin\theta}\frac{\partial\xi_r}{\partial\phi} + \frac{1}{2}\frac{\partial\xi_\phi}{\partial r} - \frac{\xi_\phi}{2r} \\ \Sigma_{r\theta} &= \Sigma\theta r = \frac{1}{2}\frac{\partial\xi_\theta}{\partial r} - \frac{\xi_\theta}{2r} + \frac{1}{2r}\frac{\partial\xi_r}{\partial\theta}. \end{aligned} \tag{3}$$

Equation (11.48) for the components of the gradient can be understood as follows: In cylindrical or spherical coordinates, the components T_{ij} can change from point to point as a result of two things: a change of the tensor $\mathbf{T}$, or the turning of the basis vectors. The two connection coefficient terms in Eq. (11.48) remove the effects of the basis turning, leaving in $T_{ij;m}$ only the influence of the change of $\mathbf{T}$ itself. There are two correction terms corresponding to the two slots (indices) of $\mathbf{T}$; the effects of basis turning on each slot get corrected one after another. If $\mathbf{T}$ had had n slots, then there would have been n correction terms, each with the form of the two in Eq. (11.48).

These expressions for derivatives of tensors are not required to deal with the vector fields of introductory electromagnetic theory, but they are essential to manipulate the tensor fields encountered in elasticity. As we shall see in Sec. 23.3, with one further generalization, we can go on to differentiate tensors in any basis (orthonormal or non-orthonormal) in a curved spacetime, as is needed to perform calculations in general relativity.

Although the algebra of evaluating the components of derivatives such as (11.48) in explicit form (e.g., in terms of $\{r, \theta, \phi\}$) can be long and tedious when done by hand, in the modern era of symbolic manipulation via computers (e.g. Maple or Mathematica), the algebra can be done quickly and accurately to obtain, e.g., expressions such as Eqs. (3) of Box 11.3.

****

EXERCISES

Exercise 11.8 *Derivation and Practice: Gradient of a Second Rank Tensor*
By a computation analogous to Eq. (11.42), derive Eq. (11.48) for the components of the gradient of a second rank tensor in any orthonormal basis

Exercise 11.9 *Derivation and Practice: Connection in Spherical Coordinates*

(a) By drawing pictures analogous to Fig. 11.7, show that

$$\nabla_\phi \mathbf{e}_r = \frac{1}{r}\mathbf{e}_\phi \ , \quad \nabla_\theta \mathbf{e}_r = \frac{1}{r}\mathbf{e}_\theta \ , \quad \nabla_\phi \mathbf{e}_\theta = \frac{\cot\theta}{r}\mathbf{e}_\phi \ . \tag{11.49}$$

(b) From these relations deduce the connection coefficients (11.41).

Exercise 11.10 *Derivation and Practice: Expansion in Cylindrical and Spherical Coordinates*
Derive Eqs. (11.46) and (11.47) for the divergence of the vector field $\boldsymbol{\xi}$ in cylindrical and spherical coordinates using the connection coefficients (11.40) and (11.41).

****

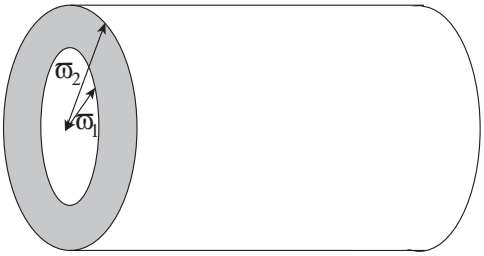

Fig. 11.8: Pipe.

11.6 T2 Solving the 3-Dimensional Elastostatic Equation in Cylindrical Coordinates: Simple Methods, Separation of Variables and Green's Functions

11.6.1 Simple Methods: Pipe Fracture and Torsion Pendulum

As an example of an elastostatic problem with cylindrical symmetry, consider a cylindrical pipe that carries a high-pressure fluid (water, oil, natural gas, ...); Fig. 11.8 How thick must the pipe's wall be to ensure that it will not burst due to the fluid's pressure? We shall sketch the solution, leaving the details to the reader in Ex. 11.11.

We suppose, for simplicity, that the pipe's length is held fixed by its support system: it does not lengthen or shorten when the fluid pressure is changed. Then by symmetry, the displacement field in the pipe wall is purely radial and depends only on radius; i.e., its only nonzero component is $\xi_\varpi(\varpi)$. The radial dependence is governed by radial force balance,

$$f_\varpi = K\Theta_{;\varpi} + 2\mu\Sigma_{\varpi j;j} = 0 \ . \tag{11.50}$$

[Eq. (11.19)].

The expansion and the components of shear that appear in this force-balance equation can be read off the cylindrical-coordinate Eq. (11.46) and Eq. (2) of Box 10.3; most importantly

$$\Theta = \frac{\partial \xi_\varpi}{\partial \varpi} + \frac{\xi_\varpi}{\varpi} \ . \tag{11.51}$$

The second term in the radial force balance equation (11.50) is proportional to $\sigma_{\varpi j;j}$ which, using Eq. (11.46) and noting that the only nonzero connection coefficients are $\Gamma_{\varpi\phi\phi} = -\Gamma_{\phi\varpi\phi} = -1/\varpi$ [Eq. (11.40)] and that symmetry requires the strain tensor to be diagonal, becomes

$$\Sigma_{\varpi j;j} = \Sigma_{\varpi\varpi,\varpi} + \Gamma_{\varpi\phi\phi}\Sigma_{\phi\phi} + \Gamma_{\phi\varpi\phi}\Sigma_{\varpi\varpi} \ . \tag{11.52}$$

Inserting the components of the strain tensor from Eq. (2) of Box 10.3 and the values of the connection coefficients and comparing the result with Expression (11.51) for the expansion, we obtain the remarkable result that $\sigma_{\varpi j;j} = \frac{2}{3}\partial\Theta/\partial\varpi$. Inserting this into the radial force balance equation (11.51), we obtain

$$f_\varpi = \left(K + \frac{4\mu}{3}\right)\frac{\partial\Theta}{\partial\varpi} = 0 \ . \tag{11.53}$$

Thus, *inside the pipe wall, the expansion vanishes* (the radial compression of the pipe material is equal and opposite to the azimuthal stretching), and correspondingly, the radial displacement must have the form [cf. Eq. (11.51)]

$$\xi_\varpi = A\varpi + \frac{B}{\varpi} \tag{11.54}$$

for some constants A and B. The values of these constants are fixed by the boundary conditions at the inner and outer faces of the pipe wall: $T_{\varpi\varpi} = P$ at $\varpi = \varpi_1$ (inner wall) and $T_{\varpi\varpi} = 0$ at $\varpi = \varpi_2$ (outer wall). Here P is the pressure of the fluid that the pipe carries and we have neglected the atmosphere's pressure on the outer face by comparison. Evaluating $T_{\varpi\varpi} = -K\Theta - 2\mu\Sigma_{\varpi\varpi}$ in terms of ξ_ϖ and inserting (11.54) and then imposing these boundary conditions, we obtain

$$A = \frac{P}{2K + 2\mu/d}\frac{\varpi_1^2}{\varpi_2^2 - \varpi_1^2}\,, \quad B = \frac{P}{2\mu}\frac{\varpi_1^2\varpi_2^2}{\varpi_2^2 - \varpi_1^2}\,. \tag{11.55}$$

The only nonvanishing components of the shear then work out to be equal to the radial strain:

$$\Sigma_{\varpi\varpi} = -\Sigma_{\phi\phi} = S_{\varpi\varpi} = \frac{\partial\xi_\varpi}{\partial\varpi} = -\frac{P}{\mu}\frac{\varpi_1^2}{\varpi_2^2 - \varpi_1^2}\left(\frac{\varpi_2^2}{2\varpi^2} - \frac{3\mu}{6K + 2\mu}\right) \tag{11.56}$$

This strain is maximal at the inner wall of the pipe; expressing it in terms of the ratio λ of the outer to the inner pipe radius $\lambda = \varpi_2/\varpi_1$ and using the values of $K = 180$GPa and $\mu = 81$GPa for steel, we bring this maximum strain into the form

$$S_{\varpi\varpi} = \frac{P}{\mu}\frac{5\lambda^2 - 2}{10(\lambda^2 - 1)}\,. \tag{11.57}$$

The pipe will break at a strain $\sim 10^{-3}$; for safety it is best to keep the actual strain smaller than this by an order of magnitude, $|S_{\varpi\varpi}| \lesssim 10^{-4}$. A typical pressure for an oil pipeline is $P \simeq 10$ atmospheres $\simeq 10^6$ Pa, compared to the shear modulus of steel $\mu = 81$ GPa, so $P/\mu \simeq 1.2 \times 10^{-5}$. Inserting this into Eq. (11.57) with $|S_{\varpi\varpi}| \lesssim 10^{-4}$, we deduce that the ratio of the pipe's outer radius to its inner radius must be $\lambda = \varpi_2/\varpi_1 \gtrsim 1.02$. If the pipe has a diameter of one meter, then its wall thickness should be at least one centimeter. This is typical of the pipes in oil pipelines.

Exercise 11.12 presents a second fairly simple example of elastostatics in cylindrical coordinates: a computation of the period of a torsion pendulum.

11.6.2 Separation of Variables and Green's Functions: Thermoelastic Noise in a LIGO Mirror

In more complicated situations that have moderate amounts of symmetry, the elastostatic equations can be solved by the same kinds of sophisticated mathematical techniques as one uses in electrostatics: separation of variables, Green's functions, complex potentials,

or integral transform methods; see, e.g. Gladwell (1980). We provide an example in this section, focusing on separation of variables and Green's functions.

Our example is chosen as one that makes contact with things we have already learned in optics (gravitational-wave interferometers; Sec. 8.5) and in statistical physics (the fluctuation-dissipation theory; Sec. 5.6). This application is the computation of *thermoelastic noise* in second-generation gravitational-wave detectors such as Advanced LIGO. Our analysis is based on Braginsky, Gorodetsky and Vyatchanin (1999); see also Liu and Thorne (2000).

Thermoelastic Context for the Elastostatic Problem to be Solved

We discussed laser interferometer gravitational-wave detectors in Sec. 5.6 (see especially Fig. 8.11). Recall that in such a detector, a gravitational wave moves four test-mass mirrors relative to each other, and laser interferometry is used to monitor the resulting oscillatory changes in the mirror separations. As we discussed in Sec. 5.6.1, the separations actually measured are the differences in the mirrors' generalized coordinates q, each of which is the longitudinal position ξ_z of the test mass's mirrored front face, weighted by the laser beam's Gaussian-shaped intensity distribution and averaged over the mirror's face:

$$q = \int \frac{e^{-\varpi^2/\varpi_o^2}}{\pi\varpi_o^2} \xi_z(\varpi,\phi)\varpi d\phi d\varpi \tag{11.58}$$

[Eq. (5.61) with a change of notation]. Here (ϖ, ϕ, z) are cylindrical coordinates with the axis $\varpi = 0$ along the center of the laser beam, $\varpi_o \sim 4$ cm is the radius at which the light's intensity has dropped by a factor $1/e$, and $\xi_z(\varpi,\phi)$ is the longitudinal displacement of the mirror face. The gravitational-wave signal is the difference of mirror positions divided by the interferometer arm length $L = 4$ km: $h(t) = \{[q_1(t) - q_2(t)] - [q_3(t) - q_4(t)]\}/L$, where the subscripts label the four mirrors. The thermoelastic noise is uncorrelated between the four test masses and, because the test masses and the beam spots on them are identical, it is the same in all four test masses—which means that the spectral densities of their noises add incoherently, giving

$$S_h(f) = \frac{4S_q(f)}{L^2} \ . \tag{11.59}$$

Here $S_q(f)$ is the spectral density of the fluctuations of the generalized coordinate q of any one of the test masses.

The thermoelastic noise is a variant of *thermal noise*; it arises when fluctuations of the thermal energy distribution inside a test mass randomly cause a slight increase (or decrease) in the test-mass temperature near the laser beam spot, and a corresponding thermal expansion (or contraction) of the test-mass material near the beam spot. This random expansion (or contraction) entails a displacement ξ_z of the test-mass surface and a corresponding random change of the generalized coordinate q [Eq. (11.58)].

In Ex. 11.14 we use the fluctuation-dissipation theorem (Sec. 5.6) to derive the following prescription for computing the spectral density $S_q(f)$ of these random thermoelastic fluctuations of q. Our prescription is expressed in terms of a thought experiment: Imagine applying a static, normal (z-directed) force F_o to the face of the test mass at the location of the beam spot, with the force distributed spatially with the same Gaussian profile as q so the applied stress is

$$T_{zz}^{\rm applied} = \frac{e^{-\varpi^2/\varpi_o^2}}{\pi\varpi_o^2} F_o \ . \tag{11.60}$$

This applied stress induces a strain distribution $\mathbf{S}$ inside the test mass, and that strain includes an expansion $\Theta(\varpi, \phi, z)$. The analysis in Ex. 11.14 shows that the spectral density of thermoelastic noise is expressible as follows in terms of an integral over the squared gradient of this expansion:

$$S_q(f) = \frac{2\kappa_{\rm th} E^2 \alpha^2 k T^2}{(1-2\nu)^2 C_V^2 \rho^2 F_o^2 (2\pi f)^2} \left\langle \int (\boldsymbol{\nabla}\Theta)^2 \varpi d\phi d\varpi dz \right\rangle \ . \tag{11.61}$$

Here $\kappa_{\rm th}$ is the coefficient of thermal conductivity (Sec. 2.7), E is Young's modulus, ν is the Poisson ratio, α is the coefficient of linear thermal expansion (fractional change of length induced by a unit change of temperature), T is temperature, C_V is the specific heat per unit mass at constant volume, ρ is the density, and f is the frequency at which the noise is being evaluated.

The computation of the thermoelastic noise, thus, boils down to computing the distribution $\Theta(\varpi, \phi, z, t)$ of expansion induced by the applied stress (11.60), and then evaluating the integral in Eq. (11.61). The computation is made easier by the fact that Θ and $\boldsymbol{\nabla}\Theta$ are concentrated in a region of size $\sim \varpi_o \sim 4$ cm, which is small compared to the test-mass radius and length (~ 16 cm), so in our computation we can idealize the test mass as having infinite radius and length (i.e., as being an "infinite half space" or "half-infinite body").[5]

Equations of Elasticity in Cylindrical Coordinates, and their Solution

Because the applied stress is cylindrical, the induced strain and expansion will also be cylindrical, and are thus computed most easily using cylindrical coordinates.

One way to compute the expansion Θ is to solve the zero-internal-force equation $\mathbf{f} = (K + \frac{1}{3}\mu)\boldsymbol{\nabla}(\boldsymbol{\nabla}\cdot\boldsymbol{\xi}) + \mu\nabla^2\boldsymbol{\xi} = 0$ for the cylindrical components $\xi_\varpi(z, \varpi)$ and $\xi_z(z, \varpi)$ of the displacement (a problem in elastostatics), and then evaluate the divergence $\Theta = \boldsymbol{\nabla}\cdot\boldsymbol{\xi}$. (The component ξ_ϕ vanishes by symmetry.) It is straightforward, using the techniques of Sec. 11.5, to compute the cylindrical components of $\mathbf{f}$. Reexpressing the bulk and shear moduli K and μ in terms of Young's modulus E and Poisson's ratio ν [Eq. (11.34)] and setting the internal forces to zero, we obtain

$$f_\varpi = \frac{E}{2(1+\nu)(1-2\nu)} \left[2(1-\nu)\left(\frac{\partial^2\xi_\varpi}{\partial\varpi^2} + \frac{1}{\varpi}\frac{\partial\xi_\varpi}{\partial\varpi} - \frac{\xi_\varpi}{\varpi^2}\right) + (1-2\nu)\frac{\partial^2\xi_\varpi}{\partial z^2} + \frac{\partial^2\xi_z}{\partial z\partial\varpi}\right] = 0 \ , \tag{11.62a}$$

$$f_z = \frac{E}{2(1+\nu)(1-2\nu)} \left[(1-2\nu)\left(\frac{\partial^2\xi_z}{\partial\varpi^2} + \frac{1}{\varpi}\frac{\partial\xi_z}{\partial\varpi}\right) + 2(1-\nu)\frac{\partial^2\xi_z}{\partial z^2} + \frac{\partial^2\xi_\varpi}{\partial z\partial\varpi} + \frac{1}{\varpi}\frac{\partial\xi_\varpi}{\partial z}\right] = 0 \ . \tag{11.62b}$$

These are two coupled, linear, second-order differential equations for the two unknown components of the displacement vector. As with the analogous equations of electrostatics and magnetostatics, these can be solved by separation of variables, i.e. by setting $\xi_\varpi = R(\varpi)Z(z)$

[5] Finiteness of the test mass turns out to increase $S_q(f)$ by about 20 per cent (Liu and Thorne, 2000).

and inserting into Eq. (11.62a). We seek solutions that die out at large ϖ and z. The general variables-separated solutions of this sort are

$$\xi_\varpi = \int_0^\infty [\alpha(k) - (2 - 2\nu - kz)\beta(k)]\, e^{-kz} J_1(k\varpi) k dk \ ,$$
$$\xi_z = \int_0^\infty [\alpha(k) + (1 - 2\nu + kz)\beta(k)]\, e^{-kz} J_0(k\varpi) dk \ , \tag{11.63}$$

where J_0 and J_1 are Bessel functions of order 0 and 1.

Boundary Conditions

The functions $\alpha(k)$ and $\beta(k)$ are determined by boundary conditions on the face of the test mass: The force per unit area exerted across the face by the strained test-mass material, T_{zj} at $z = 0$ with $j = \{\varpi, \phi, z\}$, must be balanced by the applied force per unit area, $T_{zj}^{\rm applied}$ [Eq. (11.60)]. The (shear) forces in the ϕ direction, $T_{z\phi}$ and $T_{z\phi}^{\rm applied}$, vanish because of cylindrical symmetry and thus provide no useful boundary condition. The (shear) force in the ϖ direction, which must vanish since $T_{z\varpi}^{\rm applied} = 0$, is given by [cf. Eq. (2) in Box 11.3]

$$T_{z\varpi}(z=0) = -2\mu\Sigma_{z\varpi} = -\mu\left(\frac{\partial\xi_z}{\partial\varpi} + \frac{\partial\xi_\varpi}{\partial z}\right) = -\mu\int_0^\infty [\beta(k) - \alpha(k)]\, J_1(kz) k dk = 0 \ , \tag{11.64}$$

which implies that $\beta(k) = \alpha(k)$. The (normal) force in the z direction, which must balance the applied normal force, is $T_{zz} = -K\Theta - 2\mu\Sigma_{zz}$; using Eq. (2) in Box 11.3 and Eqs. (11.63), this reduces to

$$T_{zz}(z=0) = -2\mu\int_0^\infty \alpha(k) J_0(k\varpi) k dk = T_{zz}^{\rm applied} = \frac{e^{-\varpi^2/\varpi_o^2}}{\pi\varpi_o^2} F_o \cos(2\pi f t) \ , \tag{11.65}$$

which can be inverted[6] to give

$$\alpha(k) = \beta(k) = -\frac{1}{4\pi\mu} e^{-k^2\varpi_o^2/4} F_o \cos(2\pi f t) \ . \tag{11.66}$$

Inserting this into the Eqs. (11.63) for the displacement, and then evaluating the expansion $\Theta = \boldsymbol{\nabla}\cdot\boldsymbol{\xi} = \xi_{z,z} + \varpi^{-1}(\varpi\xi_\varpi)_{,\varpi}$, we obtain

$$\Theta = -4\nu\int_0^\infty \alpha(k) e^{-kz} J_0(k\varpi) k dk \ . \tag{11.67}$$

Side Remark: As in electrostatics and magnetostatics, so also in elasticity theory, one can solve an elastostatics problem using Green's functions instead of separation of variables. We explore this, for our applied Gaussian force, in Ex. 11.15 below. For greater detail on Green's functions in elastostatics and their applications, from an engineer's viewpoint, see Johnson (1985). For other commonly used solution techniques see, e.g. Gladwell (1980).

Noise Spectral Density

[6] The inversion and the subsequent evaluation of the integral of $(\boldsymbol{\nabla}\Theta)^2$ are aided by the following expressions for the Dirac delta function: $\delta(k-k') = k\int_0^\infty J_0(k\varpi)J_0(k'\varpi)\varpi d\varpi = k\int_0^\infty J_1(k\varpi)J_1(k'\varpi)\varpi d\varpi$.

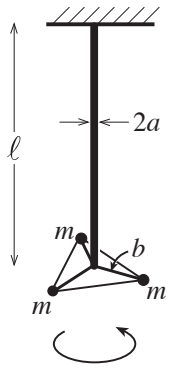

Fig. 11.9: Torsion Pendulum

It is now straightforward to compute the gradient of this expansion, square and integrate to get the spectral density $S_q(f)$ [Eq. (11.61)]. That result, when inserted into Eq. (11.59) gives, for the gravitational-wave noise,

$$S_h(f) = \frac{32(1+\nu)^2\kappa_{\rm th}\alpha^2 kT^2}{\sqrt{2\pi}C_V^2\rho^2\varpi_o^3(2\pi f)^2} \ . \tag{11.68}$$

A possible material for the test masses is sapphire, for which $\nu = 0.29$, $\kappa_{\rm th} = 40$ W m^{-1} K^{-1}, $\alpha = 5.0 \times 10^{-6}$ K^{-1}, $C_V = 790$ J kg^{-1} K^{-1}, $\rho = 4000$ kg m^{-3}. Inserting these into Eq. (11.68), along with the interferometer arm length $L = 4$ km, a laser-beam radius $\varpi_o = 40$ mm, and room temperature $T = 300$ K, we obtain the following result for the thermoelastic gravity-wave noise in a bandwidth equal to frequency:

$$\sqrt{fS_h(f)} = 2.6 \times 10^{-23}\sqrt{\frac{100{\rm Hz}}{f}} \ . \tag{11.69}$$

We shall explore the consequences of this noise for gravitational-wave detection in Chap. 26.

****

EXERCISES

Exercise 11.11 *Derivation and Practice: Fracture of a Pipe*
Fill in the details of the text's analysis of the deformation of a pipe carrying a high-pressure fluid, and the wall thickness required to protect the pipe against fracture, Sec. 11.6.1.

Exercise 11.12 *Practice: Torsion pendulum*
A torsion pendulum is a very useful tool for performing the classical Eötvös experiment and for seeking evidence for hypothetical *fifth* (not to mention *sixth*) forces (see, e.g., Will 1993 and references therein, or Fig. 1.6 of Misner, Thorne and Wheeler 1973). It would be advantageous to design a torsion pendulum with a one day period (Figure 11.9). In this exercise we shall estimate whether this is possible. The pendulum consists of a thin cylindrical wire of length l and radius a. At the bottom of the wire are suspended three masses at the corners of an equilateral triangle at a distance b from the wire.

(a) Show that the longitudinal strain is

$$\xi_{z;z} = \frac{3mg}{\pi a^2 E} \, . \tag{11.70a}$$

(b) What component of shear is responsible for the restoring force in the wire, which causes torsion pendulum to oscillate?

(c) Show that the pendulum undergoes torsional oscillations with period

$$P = 2\pi \left(\frac{\ell}{g}\right)^{1/2} \left(\frac{2b^2 E \xi_{z;z}}{a^2 \mu}\right)^{1/2} \tag{11.70b}$$

(d) Do you think you could design a pendulum that attains the goal of a one day period?

Exercise 11.13 *Derivation and Practice: Evaluation of Elastostatic Force in Cylindrical Coordinates*
Derive Eqs. (11.62) for the cylindrical components of the internal elastostatic force per unit volume $\mathbf{f} = (K + \frac{1}{3}\mu)\boldsymbol{\nabla}(\boldsymbol{\nabla}\cdot\boldsymbol{\xi}) + \mu\nabla^2\boldsymbol{\xi}$ in a cylindrically symmetric situation.

Exercise 11.14 *Derivation and Example: Thermoelastic Noise*
Derive Eq. (11.61) for the thermoelastic noise in a gravitational-wave test mass by the following steps: First, read the discussion of the fluctuation-dissipation theorem in Sec. 5.6, and then read Ex. 5.7, which is the starting point for the derivation. Our $S_q(f)$ is given by Eq. (5.70). The key unknown quantity in this equation is the dissipation rate $W_{\rm diss}$ associated with a sinusoidally oscillating applied stress [Eq. (11.60), multiplied by $\cos(2\pi f t)$].

(a) There are three important time scales in this problem: (i) the oscillation period of the applied stress $\tau_{\rm applied} = 1/f \sim 0.01$ s, (ii) the time $\tau_{\rm sound}$ for sound waves to travel across the test mass (a distance ~ 14 cm; the sound speed, as we shall see in Chap. 11, is roughly $\sqrt{E/\rho}$), and (iii) the time $\tau_{\rm heat}$ for diffusive heat conductivity to substantially change the temperature distribution inside the test mass (cf. the discussion of heat conductivity in Sec. 2.7). Estimate, roughly, $\tau_{\rm sound}$ and $\tau_{\rm heat}$, and thereby show that $\tau_{\rm sound} \ll \tau_{\rm applied} \ll \tau_{\rm heat}$. Explain why this means that in evaluating $W_{\rm diss}$, we can (i) treat the test-mass strain as being produced quasistatically (i.e., we can ignore the inertia of the test-mass material), and (ii) we can treat the expansion of the test-mass material adiabatically (i.e., ignore the effects of heat flow when computing the temperature distribution in the test mass).

(b) Show that, when the test-mass material adiabatically expands by an amount $\Delta V/V = \Theta$, its temperature goes down by

$$\delta T = \frac{-\alpha E T}{C_V \rho (1-2\nu)} \Theta \, . \tag{11.71}$$

For a textbook derivation of this, see Sec. 6 of Landau and Lifshitz (1986). In that section a clean distinction is made between the bulk modulus K for expansions at

constant temperature and that $K_{\rm ad}$ for adiabatic expansion. For most materials, these bulk moduli are nearly the same; for example, for sapphire they differ by only ~ 1 part in 10^5 [cf. Eqs. (6.7), (6.8) of Landau and Lifshitz (1986) and the numbers for sapphire at the end of Sec. 11.6.2; and note the difference of notation: α of this paper is 1/3 that of Landau and Lifshitz, and $C_V\rho$ of this paper is C_V of Landau and Lifshitz].

(c) The inhomogeneity of the expansion Θ causes the temperature perturbation δT to be inhomogeneous, and that inhomogeneity produces a heat flux $\mathbf{q} = -\kappa_{\rm th}\boldsymbol{\nabla}\delta T$. Whenever an amount Q of heat flows from a region of high temperature T to one of slightly lower temperature $T - dT$, there is an increase of entropy, $dS = Q/(T-dT) - Q/T = QdT/T^2$. Show that for our situation, the resulting rate of entropy increase per unit volume is

$$\frac{dS}{dVdt} = \frac{-\mathbf{q}\cdot\boldsymbol{\nabla}\delta T}{T^2} = \frac{\kappa_{\rm th}\cdot(\boldsymbol{\nabla}\delta T)^2}{T^2}\ . \tag{11.72}$$

(We shall rederive this fundamental result from a different viewpoint in Part IV.)

(d) This entropy increase entails a creation of new thermal energy at a rate per unit volume $dE_{\rm th}/dVdt = TdS/dVdt$. Since, for our thought experiment with temporally oscillating applied stress, this new thermal energy must come from the oscillating elastic energy, the rate of dissipation of elastic energy must be

$$W_{\rm diss} = \int \kappa_{\rm th}(\boldsymbol{\nabla}\delta T)^2 T dV\ . \tag{11.73}$$

By combining with Eq. (11.71), inserting into Eq. (5.70) and averaging over the period $\tau_{\rm applied}$ of the applied force, derive Eq. (11.61) for $S_q(f)$. Explain why, in this equation, we can treat the applied force as static rather than oscillatory, which is what we did in the text.

Exercise 11.15 **** Example: Green's Function for Normal Force on Half-Infinite Body*
Suppose that a stress $T^{\rm applied}_{zj}(\mathbf{x}_o)$ is applied on the face $z = 0$ of a half-infinite elastic body (one that fills the region $z > 0$). Then by virtue of the linearity of the elastostatics equation $\mathbf{f} = (K + \frac{1}{3}\mu)\boldsymbol{\nabla}(\boldsymbol{\nabla}\cdot\boldsymbol{\xi}) + \mu\nabla^2\boldsymbol{\xi} = 0$ and the linearity of its boundary conditions, $T^{\rm internal}_{zj} = T^{\rm applied}_{zj}$, there must be a Green's function $G_{jk}(\mathbf{x}-\mathbf{x}_o)$ such that the body's internal displacement $\boldsymbol{\xi}(\mathbf{x})$ is given by

$$\boxed{\xi_j(\mathbf{x}) = \int G_{jk}(\mathbf{x}-\mathbf{x}_0)T^{\rm applied}_{zk}(\mathbf{x}_o)d^2x_o\ .} \tag{11.74}$$

Here the integral is over all points $\mathbf{x}_o$ on the face of the body ($z = 0$), and $\mathbf{x}$ can be anywhere inside the body, $z \geq 0$.

(a) Show that, if a force F_j is applied on the body's surface at a single point, the origin of coordinates, then the displacement inside the body is

$$\xi_j(\mathbf{x}) = G_{jk}(\mathbf{x})F_k\ . \tag{11.75}$$

Thus, the Green's function can be thought of as the body's response to a point force on its surface.

(b) As a special case, consider a point force F_z directed perpendicularly into the body. The resulting displacement turns out to have cylindrical components[7]

$$\begin{aligned} \xi_z &= G_{zz}(\varpi, z)F_z = \frac{1+\nu}{2\pi E}\left[\frac{2(1-\nu)}{\varpi} + \frac{z^2}{\varpi^3}\right]F_z \ , \\ \xi_\varpi &= G_{\varpi z}(\varpi, z)F_z = -\frac{(1+\nu)(1-2\nu)}{2\pi E}\frac{F_z}{\varpi} \ . \end{aligned} \tag{11.76}$$

It is straightforward to show that this displacement does satisfy the elastostatics equations (11.62). Show that it also satisfies the required boundary condition $T_{z\varpi}(z=0) = -2\mu\Sigma_{z\varpi} = 0$.

(c) Show that for this displacement, $T_{zz} = -K\Theta - 2\mu\Sigma_{zz}$ vanishes everywhere on the body's surface $z = 0$ except at the origin $\varpi = 0$ and is infinite there. Show that the integral of this normal stress over the surface is F_z, and therefore $T_{zz}(z=0) = F_z\delta_2(\mathbf{x})$ where δ_2 is the two-dimensional Dirac delta function in the surface. This is the second required boundary condition

(d) Plot the integral curves of the displacement vector $\boldsymbol{\xi}$ (i.e. the curves to which $\boldsymbol{\xi}$ is parallel) for a reasonable choice of Poisson's ratio ν. Explain physically why the curves have the form you find.

(e) One can use the Green's function (11.76) to compute the displacement $\boldsymbol{\xi}$ induced by the Gaussian-shaped pressure (11.60) applied to the body's face, and to then evaluate the induced expansion and thence the thermoelastic noise; see Braginsky, Gorodetsky and Vyatchanin (1999), or Liu and Thorne (2000). The results agree with those (11.67) and (11.68) deduced using separation of variables.

****

11.7 Reducing the Elastostatic Equations to One Dimension for a Bent Beam; Cantilever Bridges

When dealing with bodies that are much thinner in two dimensions than the third (e.g. rods, wires, and beams), one can use the *method of moments* to reduce the three-dimensional elastostatic equations to ordinary differential equations in one dimension (a process called *dimensional reduction*). We have already met an almost trivial example of this in our discussion of Hooke's law and Young's modulus (Sec. 11.4 and Fig. 11.1). In this section we shall discuss a more complicated example, the bending of a beam through a small displacement angle; and in Ex. 11.17 we shall analyze a more complicated example: the bending of a very long, elastic wire into a complicated shape called an *elastica*.

[7]For the other components of the Green's function, written in Cartesian coordinates (since a non-normal applied force breaks the cylindrical symmetry), see Eqs. (8.18) of Landau and Lifshitz (1986).

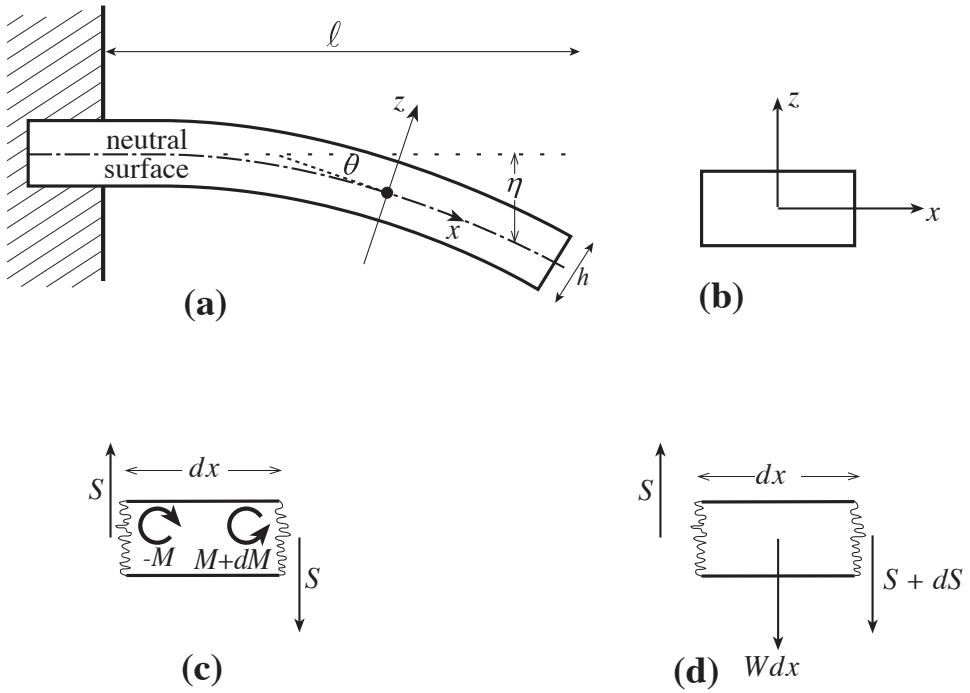

Fig. 11.10: Bending of a cantilever. a) A beam is held rigidly at one end and extends horizontally with the other end free. We introduce an orthonormal coordinate system (x, y, z) with $\mathbf{e}_x$ extending along the beam. We only consider small departures from equilibrium. The bottom of the beam will be compressed, the upper portion extended. There is therefore a neutral surface $z = 0$ on which the strain $\xi_{x,x}$ vanishes. b) The beam shown here has rectangular cross section with horizontal width w, vertical thickness h and length ℓ. c) The bending torque M must be balanced by the torque exerted by the vertical shearing force S. d) S must vary along the beam so as to support the beam's weight per unit length, W.

Our beam-bending example is motivated by a common method of bridge construction, which uses cantilevers. (A famous historical example is the old bridge over the Firth of Forth in Scotland that was completed in 1890 with a main span of half a km.) The principle is to attach two independent beams to the two shores and allow them to meet in the middle. (In practice the beams are usually supported at the shores on piers and strengthened along their lengths with trusses.)

Let us make a simple model of a cantilever (Figure 11.10). Consider a beam clamped rigidly at one end, with length ℓ, horizontal width w and vertical thickness h. Introduce local cartesian coordinates with $\mathbf{e}_x$ pointing along the beam and $\mathbf{e}_z$ pointing vertically upward. Imagine the beam extending horizontally in the absence of gravity. Now let it sag under its own weight so that each element is displaced through a small distance $\boldsymbol{\xi}(\mathbf{x})$. The upper part of the beam is stretched while the lower part is compressed, so there must be a *neutral surface* where the horizontal strain $\xi_{x,x}$ vanishes. This neutral surface must itself be curved downward. Let its downward displacement from the horizontal plane that it occupied before sagging be $\eta(x)(> 0)$, let a plane tangent to the neutral surface make an angle $\theta(x)$ (also > 0) with the horizontal, and adjust the x and z coordinates so x runs along the slightly

curved neutral plane and z is orthogonal to it (Fig. 11.10). The longitudinal strain is then given to first order in small quantities by

$$\xi_{x,x} = \frac{z}{\mathcal{R}} = z\frac{d\theta}{dx} \simeq z\frac{d^2\eta}{dx^2} \ , \tag{11.77}$$

where $\mathcal{R} = dx/d\theta > 0$ is the radius of curvature of the beam's bend and we have chosen $z = 0$ at the neutral surface. The one-dimensional displacement $\eta(x)$ will be the focus of dimensional reduction of the elastostatic equations.

As in our discussion of Hooke's law for a stretched rod (Sec. 11.4), we can regard the beam as composed of a bundle of long parallel fibers, stretched along their length and free to contract transversely. The longitudinal stress is therefore

$$T_{xx} = -E\xi_{x,x} = -Ez\frac{d^2\eta}{dx^2}. \tag{11.78}$$

We can now compute the horizontal force density, which must vanish in elastostatic equilibrium[8]

$$f_x = -T_{xx,x} - T_{xz,z} = Ez\frac{d^3\eta}{dx^3} - T_{xz,z} = 0. \tag{11.79}$$

This is a partial differential equation. We convert it into a one-dimensional ordinary differential equation by the *method of moments*: We multiply it by z and integrate over z (i.e., we compute its "first moment"). Integrating the second term, $\int zT_{xz,z}dz$, by parts and using the boundary condition $T_{xz} = 0$ on the upper and lower surfaces of the beam, we obtain

$$\frac{Eh^3}{12}\frac{d^3\eta}{dx^3} = -\int_{-h/2}^{h/2} T_{xz}dz \ . \tag{11.80}$$

Notice (using $T_{xz} = T_{zx}$) that the integral, when multiplied by the beam's width w in the y direction, is the vertical *shearing force* $S(x)$ in the beam:

$$\boxed{S = \int T_{zx}dydz = w\int_{-h/2}^{h/2} T_{zx}dz = -D\frac{d^3\eta}{dx^3} \ .} \tag{11.81}$$

Here

$$\boxed{D \equiv E\int z^2 dydz = Ewh^3/12} \tag{11.82}$$

is called the beam's *flexural rigidity*. Notice that it is the second moment of the beam's Young's modulus.

As an aside, we can gain some insight into Eq. (11.81) by examining the torques that act on a segment of the beam with length dx. As shown in Fig. 11.10c, the shear forces on

[8]Because the coordinates are curvilinear, there are connection coefficient terms in this equation that have been omitted: $-\Gamma_{xjk}T_{jk} - \Gamma_{jkj}T_{xk}$. However each Γ has magnitude $1/\mathcal{R}$ so these terms are of order $T_{jk}/\mathcal{R}$, whereas the terms kept in Eq. (11.79) are of order T_{xx}/ℓ and T_{xz}/h; and since the thickness h and length ℓ of the beam are small compared to the beam's radius of curvature $\mathcal{R}$, the connection-coefficient terms are negligible.

the two ends of the segment exert a clockwise torque $2S(dx/2) = Sdx$. This is balanced by a counterclockwise torque due to the stretching of the upper half of the segment and compression of the lower half, i.e. due to the bending of the beam. This bending torque is

$$\boxed{M \equiv \int T_{xx} z dy dz = -D \frac{d^2\eta}{dx^2}} \tag{11.83}$$

on the right end of the segment and minus this on the left, so torque balance says $(dM/dx)dx = Sdx$, i.e.

$$S = dM/dx \ . \tag{11.84}$$

This is precisely Eq. (11.81).

Equation (11.81) [or equivalently (11.84)] embodies half of the elastostatic equations. It is the x component of force balance $f_x = 0$, converted to an ordinary differential equation by evaluating its lowest non-vanishing moment: its first moment, $\int z f_x dy dz = 0$ [Eq. (11.80)]. The other half is the z component of stress balance, which we can write as

$$T_{zx,x} + T_{zz,z} + \rho g = 0 \tag{11.85}$$

(vertical elastic force balanced by gravitational pull on the beam). We can convert this to a one-dimensional ordinary differential equation by taking its lowest nonvanishing moment, its zero'th moment, i.e. by integrating over y and z. The result is

$$\frac{dS}{dx} = -W \ , \tag{11.86}$$

where $W = g\rho wh$ is the beam's weight per unit length.

Combining our two dimensionally reduced components of force balance, Eqs. (11.81) and (11.86), we obtain a fourth order differential equation for our one-dimensional displacement $\eta(x)$:

$$\boxed{\frac{d^4\eta}{dx^4} = \frac{W}{D} \ .} \tag{11.87}$$

(Fourth order differential equations are characteristic of elasticity.)

Equation (11.87) can be solved subject to four appropriate boundary conditions. However, before we solve it, notice that for a beam of a fixed length ℓ, the deflection η is inversely proportional to the flexural rigidity. Let us give a simple example of this scaling. American floors are conventionally supported by wooden *joists* of 2" (inch) by 6" lumber with the 6" side vertical. Suppose an inept carpenter installed the joists with the 6" side horizontal. The flexural rigidity of the joist would be reduced by a factor 9 and the center of the floor would be expected to sag 9 times as much as if the joists had been properly installed – a potentially catastrophic error.

Also, before solving Eq. (11.87), let us examine the approximations that we have made. First, we have assumed that the sag is small compared with the length of the beam in making the small angle approximation in Eq. (11.77), and we have assumed the beam's radius of curvature is large compared to its length in neglecting connection coefficient terms

(footnote 8). These will usually be the case, but are not so for the elastica studied in Ex. 11.17. Second, by using the method of moments rather than solving for the complete local stress tensor field, we have ignored the effects of some components of the stress tensor. In particular, in evaluating the bending torque [Eq. (11.83)] we have ignored the effect of the T_{zx} component of the stress tensor. This is $O(h/\ell)T_{xx}$ and so our equations can only be accurate for fairly slender beams. Third, the extension above the neutral surface and the compression below the neutral surface lead to changes in the cross sectional shape of the beam. The fractional error here is of order the longitudinal shear, which is small for real materials.

The solution to Eq. (11.87) is a fourth order polynomial with four unknown constants to be set by boundary conditions. In this problem, the beam is held horizontal at the fixed end so that $\eta(0) = \eta'(0) = 0$, where $' = d/dx$. At the free end, T_{zx} and T_{xx} must vanish, so the shearing force S must vanish, whence $\eta'''(\ell) = 0$ [Eq. (11.81)]; and the bending torque M [Eq. (11.83)] must also vanish, whence [by Eq. (11.84)] $\int S dx \propto \eta''(\ell) = 0$. By imposing these four boundary conditions $\eta(0) = \eta'(0) = \eta''(\ell) = \eta'''(\ell)$ on the solution of Eq. (11.87), we obtain for the beam shape

$$\eta(x) = \frac{W}{D}\left(\frac{1}{4}\ell^2 x^2 - \frac{1}{6}\ell x^3 + \frac{1}{24}x^4\right) . \tag{11.88a}$$

Therefore the end of the beam sags by

$$\eta(\ell) = \frac{W\ell^4}{8D} . \tag{11.88b}$$

Problems in which the beam rests on supports rather than is clamped can be solved in a similar manner. The boundary conditions will be altered, but the differential equation (11.87) will be unchanged.

Now suppose that we have a cantilever bridge of constant vertical thickness h and total span $2\ell \sim$100m made of material with density $\rho \sim 8 \times 10^3$kg m^{-3} (e.g. reinforced concrete) and Young's modulus $E \sim 100$GPa. Suppose further that we want the center of the bridge to sag by no more than $\eta \sim 1$m. According to Eq. (11.88b), the thickness of the beam must satisfy

$$h \gtrsim \left(\frac{3\rho g \ell^4}{2E\eta}\right)^{1/2} \sim 2.7\text{m} . \tag{11.89}$$

This estimate makes no allowance for all the extra strengthening and support present in real structures (e.g. via trusses and cables) and so it is an overestimate.

****

EXERCISES

Exercise 11.16 *Derivation: Sag in a cantilever*

(a) Verify Eqs. (11.88) for the sag in a horizontal beam clamped at one end and allowed to hang freely at the other end.

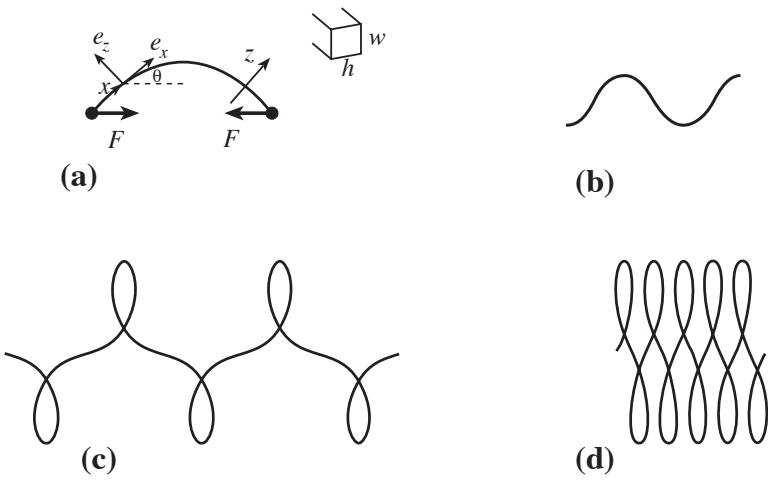

Fig. 11.11: Elastica. (a) A bent wire is in elastostatic equilibrium under the action of equal and opposite forces applied at its two ends. x measures distance along the neutral surface; z measures distance orthogonal to the wire in the plane of the bend. (b), (c), (d) Examples of the resulting shapes.

(b) Now consider a similar beam with constant cross section and loaded with weights so that the total weight per unit length is $W(x)$. Give a Green's function for the sag of the free end in terms of an integral over $W(x)$.

Exercise 11.17 **** Example: Elastica*
Consider a slender wire of rectangular cross section resting on a horizontal surface (so gravity is unimportant), with horizontal thickness h and vertical thickness w. Let the wire be bent in the horizontal plane (so gravity is unimportant) as a result of equal and opposite forces F that act at its ends; Fig. 11.11. The various shapes the wire can assume are called *elastica*; they were first computed by Euler in 1744 and are discussed on pp. 401–404 of Love (1927). The differential equation that governs the wire's shape is similar to that for the cantilever, Eq. (11.87), with the simplification that the wire's weight does not enter the problem and the complication that the wire is long enough to deform through large angles.
It is convenient (as in the cantilever problem, Fig. 11.10) to introduce curvilinear coordinates with coordinate x measuring distance along the neutral surface, z measuring distance orthogonal to x in the plane of the bend (horizontal plane), and y measured perpendicular to the bending plane (vertically). The unit vectors along the x, y, and z directions are $\mathbf{e}_x$, $\mathbf{e}_y$, $\mathbf{e}_z$ (Figure 11.11). Let $\theta(x)$ be the angle between $\mathbf{e}_x$ and the applied force $\mathbf{F}$; $\theta(x)$ is determined, of course, by force and torque balance.

(a) Show that force balance along the x and z directions implies

$$F\cos\theta = \int T_{xx}dydz\ , \quad F\sin\theta = \int T_{zx}dydz \equiv S\ . \tag{11.90a}$$

(b) Show that torque balance for a short segment of wire implies

$$S = \frac{dM}{dx} , \qquad \text{where } M(x) \equiv \int zT_{xx}dydz \text{ is the bending torque.} \tag{11.90b}$$

(c) Show that the stress-strain relation in the wire implies

$$M = -D\frac{d\theta}{dx} , \tag{11.90c}$$

where $D = Ewh^3/12$ is the flexural rigidity, Eq. (11.82).

(d) From the above relations, derive the following differential equation for the shape of the wire:

$$\boxed{\frac{d^2\theta}{dx^2} = -\frac{F\sin\theta}{D} .} \tag{11.90d}$$

This is the same equation as desribes the motion of a simple pendulum!

(e) Go back through your analysis and identify any place that connection coefficients would enter into a more careful computation, and explain why the connection-coefficient terms are neglible.

(f) Find one non-trivial solution of the elastica equation (11.90d) either analytically using elliptic integrals or numerically. (The general solution can be expressed in terms of elliptic integrals.)

(g) Solve analytically or numerically for the shape adopted by the wire corresponding to your solution in (f), in terms of Cartesian coordinates (X, Z) in the bending (horizontal) plane. Hint: express the curvature of the wire, $1/\mathcal{R} = d\theta/dx$ as

$$\frac{d\theta}{dx} = \frac{d^2X}{dZ^2}\left[1 + \left(\frac{dX}{dZ}\right)^2\right]^{-3/2} . \tag{11.90e}$$

(h) Obtain a uniform piece of wire and adjust the force $\mathbf{F}$ to compare your answer with experiment.

Exercise 11.18 *Example: Foucault Pendulum*
In the design of a Foucault pendulum for measuring the earth's general relativistic "gravitomagnetic field" (discussed further in Part VI), it is crucial that the pendulum's restoring force be isotropic, since anisotropy will make the swinging period be different in different planes and thereby will cause precession of the plane of swing (Braginsky, Polnarev and Thorne 1984). The answer to the elastica exercise 11.17 can be adapted to model the effect of anisotropy on the pendulum's period.

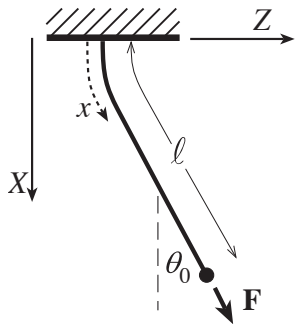

Fig. 11.12: Foucault Pendulum

(a) Consider a pendulum of mass m and length ℓ suspended as shown in Figure 11.12 by a rectangular wire with thickness h in the plane of the bend ($X-Z$ plane) and thickness w orthogonal to that plane (Y direction). Explain why the force that the wire exerts on the mass is $-\mathbf{F} = -(mg\cos\theta_o + m\ell\dot{\theta}_o^2)\mathbf{e}_x$, where g is the acceleration of gravity, θ_o is defined in the figure, $\dot{\theta}_o$ is the time derivative of θ_o due to the swinging of the pendulum, and in the second term we have assumed that the wire is long compared to its region of bend. Express the second term in terms of the amplitude of swing $\theta_o^{\max}$, and show that for small amplitudes $\theta_o^{\max} \ll 1$, $\mathbf{F} \simeq mg\mathbf{e}_x$. Use this approximation in the subsequent parts.

(b) Assuming that all along the wire, its angle $\theta(x)$ to the vertical is small, $\theta \ll 1$, show that

$$\theta(x) = \theta_o[1 - e^{-x/\lambda}] \,, \tag{11.91a}$$

where λ (not to be confused with the Lame constant) is

$$\lambda = \frac{h}{(12\epsilon)^{1/2}} \,, \tag{11.91b}$$

$\epsilon = \xi_{x,x}$ is the longitudinal strain in the wire, and h is the wire's thickness in the plane of its bend. Note that the bending of the wire is concentrated near the support, so this is where dissipation will be most important and where most of the suspension thermal noise will arise (cf. Sec. 5.6 for discussion of thermal noise).

(c) Hence show that the shape of the wire is given in terms of cartesian coordinates by

$$Z = [X - \lambda(1 - e^{-X/\lambda})]\theta_o \,, \tag{11.91c}$$

and that the pendulum period is

$$P = 2\pi \left(\frac{\ell - \lambda}{g}\right)^{1/2} \,. \tag{11.91d}$$

(d) Finally show that the pendulum periods when swinging along $\mathbf{e}_x$ and $\mathbf{e}_y$ differ by

$$\frac{\delta P}{P} = \left(\frac{h - w}{\ell}\right)\left(\frac{1}{48\epsilon}\right)^{1/2} \,. \tag{11.91e}$$

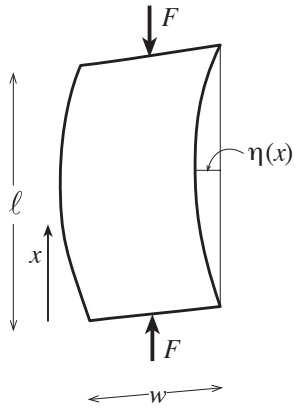

Fig. 11.13: A playing card of length ℓ, width w and thickness h is subjected to a compressive force F, applied at both ends. The ends of the card are fixed but are free to pivot.

From this one can determine how accurately the two thicknesses h and w must be equal to achieve a desired degree of isotropy in the period. A similar analysis can be carried out for the more realistic case of a slightly elliptical wire.

****

11.8 Bifurcation, Buckling and Mountain Folding

So far, we have considered stable elastostatic equilibria, and have implicitly assumed that the only reason for failure of a material is exceeding the elastic limit. However, anyone who has built a house of cards knows that mechanical equilibria can be unstable, with startling consequences. A large scale example is the formation of mountains. The surface of the earth is covered by several interlocking horizontal plates that are driven into each other by slow (hundred-million-year) convective motions in the underlying mantle. When plates are pushed together, mountains can be formed in two ways: by *folding* (e.g. the Jura Mountains of France) which sometimes happens when a portion of crust is compressed in just one direction, and by forming *domes* (e.g. the Black Hills of Dakota) which arise when there is simultaneous compression along two directions.

For a simple model of folding, take a new playing card and squeeze it between your finger and thumb (Figure 11.13). When you squeeze gently, the card remains flat, but when you gradually increase the force past a critical value $F_{\rm crit}$, the card suddenly "buckles," i.e. bends; and the curvature of the bend then increases rapidly with the applied force. For a force somewhat higher than $F_{\rm crit}$ there are equilibrium states of "higher quantum number", i.e. with one or more nodes in the transverse displacement $\eta(x)$ of the card.

To understand this quantitatively, we derive an eigenequation for the transverse displacement η as a function of distance x from one end of the card. (Although the card is effectively two dimensional, it has translation symmetry along its transverse dimension, so we can use

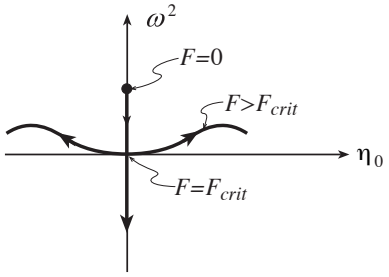

Fig. 11.14: Schematic illustration of the behavior of the frequency of small oscillations about equilibrium and the displacement of the center of the card, η_0. Equilibria with $\omega^2 > 0$ are stable; those with $\omega^2 < 0$ are unstable. The applied force F increases in the direction of the arrows.

the one-dimensional equations of the previous section.) We suppose that the ends are free to pivot but not move, so

$$\eta(0) = \eta(\ell) = 0 \ . \tag{11.92}$$

For small displacements, the bending torque of our dimensionally-reduced one-dimensional theory is [Eq. (11.83)]

$$M(x) = -D\frac{d^2\eta}{dx^2} \ , \tag{11.93}$$

where $D = wh^3E/12$ is the flexural rigidity [Eq. (11.82)]. As the card is very light (negligible gravity), the total torque around location x, acting on a section of the card from x to one end, is the bending torque applied at x plus the torque associated with the applied force $-F\eta(x)$, and this sum must vanish:

$$D\frac{d^2\eta}{dx^2} + F\eta = 0 \ . \tag{11.94}$$

The eigenfunction solutions of Eq. (11.94) satisfying boundary conditions (11.92) are

$$\eta = \eta_0 \sin kx \ , \tag{11.95a}$$

where

$$k = \left(\frac{F}{D}\right)^{1/2} = \frac{n\pi}{\ell} \quad \text{for non-negative integers } n. \tag{11.95b}$$

Therefore, there is a critical force given by

$$F_{\rm crit} = \frac{\pi^2 D}{\ell^2} = \frac{\pi^2 w h^3 E}{12\ell^2} \ , \tag{11.96}$$

below which there is no solution except $\eta = 0$ (an unbent card). When the applied force is equal to $F_{\rm crit}$, the unbent card is still a solution, and there is an additional solution (11.95) with $n = 1$ (a single arch with no nodes). The linear approximation, which we have used, cannot tell us the height η_0 of the arch as a function of F; it reports, incorrectly, that for $F = F_{\rm crit}$ all arch heights are allowed and for $F > F_{\rm crit}$ there is no solution with $n = 1$.

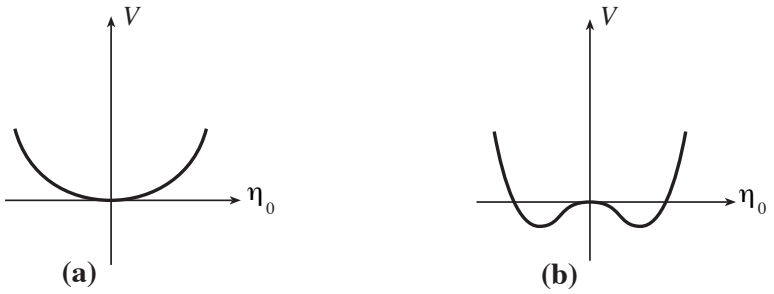

Fig. 11.15: Representation of bifurcation by a potential energy function $V(\xi_0)$. a) When the applied force is small, there is only one stable equilibrium. b) As the applied force F is increased, the bottom of the potential well flattens and eventually the number of equilibria increases from one to three, of which only two are stable.

When nonlinearities are taken into account (Ex. 11.19), the force F and the arch height η_o are related by

$$F = F_{\rm crit}\left(1 + \frac{1}{2}\sin^2(\theta_o/2) + O[\sin^4(\theta_o/2)]\right) \ , \quad \text{where } \theta_o = \frac{\pi\eta_o}{\ell} \ . \tag{11.97}$$

The sudden appearance of this new $n = 1$, arched equilibrium state as F is increased through $F_{\rm crit}$ is called a *bifurcation of equilibria*.

Bifurcations show up sharply in the elastodynamics of the playing card, as we shall see in Sec. 11.3.5: When $F < F_{\rm crit}$, small perturbations of the card's shape oscillate stably. When $F = F_{\rm crit}$, the card is neutrally stable, and its zero-frequency motion leads the card from its straight equilibrium state to its $n = 1$ bent equilibrium. When $F > F_{\rm crit}$, the straight card is an unstable equilibrium: its $n = 1$ perturbations grow in time, driving the card toward the $n = 1$ equilibrium state of Eq. (11.97).

Another nice way of looking at bifurcations is in terms of energy. Consider candidate equilibrium states labeled by the height η_0 of their arch. For each value of η_0, give the card (for concreteness) the $n = 1$ sine-wave shape $\eta = \eta_0 \sin(\pi x/\ell)$. Compute the total elastic energy $U(\eta_0)$ associated with the card's bending and subtract off the work $F\delta X$ done on the card by the applied forces F when the card arches from $\eta_0 = 0$ to height η_0. (Here $\delta X(\eta_0)$ is the arch-induced decrease in straight-line separation between card's the ends). The resulting quantity, $V(\eta_0) = U - F\delta X$ is the card's *free energy* — analogous to the Gibb's free energy $G = E - TS + PV$ of thermodynamics; it is the relevant energy for analyzing the card's equilibrium and dynamics, when the force F is continually being applied at the two ends. This free energy has the shapes shown in Fig. 11.15. At small values of the force [curve (a)], the free energy has only one minimum $\eta_0 = 0$ corresponding to a single stable equilibrium, the straight card. However, as the force is increased through $F_{\rm crit}$, the potential minimum flattens out and then becomes a maximum flanked by two new minima [curve (b)]. The maximum for $F > F_{\rm crit}$ is the unstable, zero-displacement (straight-card) equilibrium and the two minima are the two stable finite amplitude equilibria with positive and negative η_0.

This procedure of representing a continuous system with an infinite number of degrees of freedom by just one or a few coordinates and finding the equilibrium by minimizing a

free energy is quite common and powerful. Coordinates like η_0 are sometimes called *state variables*, and physical parameters like the force F are then called *control variables*.

The compressed card's bifurcation is an example of a *cusp catastrophe*; it is an analog of the catastrophes we met in geometrical optics in Sec. 6.5. Other examples of bifurcations include the failure of struts under excessive compressive loads, the instability (or *whirling*) of a drive shaft when it rotates too rapidly, and the development of triaxiality in self-gravitating fluid masses (i.e. stars) when their rotational kinetic energy becomes comparable with their gravitational energy.

Let us now return to the problem of mountain folding with which we began this section. Our playing-card model is obviously inadequate to describe the full phenomenon, as we have omitted gravitational forces and the restoring force associated with the earth's underlying *mantle*. Gravity causes no difficulties of principle as it just changes the equilibrium state. Coupling to the mantle can be modeled by treating it as an underlying viscoelastic medium. When it departs from equilibrium, the mantle changes not on a dynamical time (the time for a seismic wave to cross it, of order minutes), but instead on the time for the mantle rocks to flow, typically millions of years. Despite these limitations, our playing-card model can give a semiquantitative understanding of why plates of rock ($E \sim 100$GPa, $\nu \sim 0.25$), buckle when subjected to large, horizontal, compressive forces.

****

EXERCISES

Exercise 11.19 *Derivation and Example: Bend as a Function of Applied Force*
Derive Eq. (11.97) relating the angle $\theta_o \simeq (d\eta/dx)_{x=0} = k\eta_o = \pi\eta_o/\ell$ to the applied force F when the card has an $n = 1$, arched shape. Hint: Use the elastica differential equation $d^2\theta/dx^2 = -(F/D)\sin\theta$ [Eq. (11.90d)] for the angle between the card and the applied force at distance x from the card's end. The $\sin\theta$ becomes θ in the linear approximation used in the text; the nonlinearities embodied in the sine give rise to the desired relation. The following steps along the way toward a solution are mathematically the same as used when computing the period of a pendulum as a function of its amplitude of swing.

(a) Derive the first integral of the elastica equation

$$(d\theta/dx)^2 = 2(F/D)(\cos\theta - \cos\theta_o) \ , \tag{11.98}$$

where θ_o is an integration constant. Show that the boundary condition of no bending torque (no inflexion of the card's shape) at the card ends implies $\theta = \theta_o$ at $x = 0$ and $x = \ell$; whence $\theta = 0$ at the card's center, $x = \ell/2$.

(b) Integrate the differential equation (11.98) to obtain

$$\frac{\ell}{2} = \sqrt{\frac{D}{2F}} \int_0^{\theta_o} \frac{d\theta}{\sqrt{\cos\theta - \cos\theta_o}} \ . \tag{11.99}$$

(c) Perform the change of variable $\sin(\theta/2) = \sin(\theta_o/2)\sin\phi$ and thereby bring Eq. (11.99) into the form

$$\ell = 2\sqrt{\frac{D}{F}}\int_0^{\pi/2}\frac{d\phi}{\sqrt{1-\sin^2(\theta_o/2)\sin^2\phi}} = 2\sqrt{\frac{D}{F}}\,K[\sin^2(\theta_o/2)]\ . \tag{11.100}$$

Here $K(y)$ is the complete elliptic integral of the first type, with the parametrization used by Mathematica (which differs from many books).

(d) Expand Eq. (11.100) in powers of $\sin^2(\theta_o/2)$ to obtain

$$F = F_{\rm crit}\frac{4}{\pi^2}K^2[\sin^2(\theta_o/2)] = F_{\rm crit}\left[1+\frac{1}{2}\sin^2(\theta_o/2)+\frac{11}{32}\sin^4(\theta_o/2)+\ldots\right]\ , \tag{11.101}$$

which is our desired result (11.97).

Exercise 11.20 *Practice: The Height of Mountains*
Estimate the maximum size of a mountain by requiring that the shear stress in the underlying rocks not exceed the elastic limit. Compare your answer with the height of the tallest mountains on Earth.

Exercise 11.21 *Example: Neutron Star Crusts*
The crust of a neutron star is made of iron ($A = 56, Z = 26$) at density ρ. It is supported against the pull of gravity by the pressure of a relativistic, degenerate, electron gas (Sec. 2.5.4) whose iron ions are arranged in a body centered cubic lattice that resists shearing. Estimate the ratio of shear modulus to bulk modulus μ/K, and use this to estimate roughly the ratio of height to width of mountains on a neutron star. You might proceed as follows:

(a) Show that the electron Fermi energy is given by

$$E_F = (3\pi^2 n_e)^{1/3}\hbar c\ ,$$

where $n_e = Z\rho/Am_P$ is the free electron density. Hence show the Fermi pressure is given by

$$p_F = \frac{1}{4}n_e E_F\ .$$

(b) Use the definition of Bulk Modulus preceding Eq. (11.18) to express it in the form

$$K = \frac{1}{3}n_e E_F$$

(c) Show that the iron ions' body centered cubic lattice produces a shear modulus of magnitude

$$\mu = C\left(\frac{n_e}{Z}\right)^{4/3}Z^2e^2\ ,$$

where C is a numerical constant of order unity. Hence show that the ratio of the shear modulus to the bulk modulus is

$$\frac{\mu}{K} = \left(\frac{3}{\pi}\right)^{2/3}CZ^{2/3}\left(\frac{e^2}{\hbar c}\right)\ .$$

(d) By an order-of-magnitude analysis of stress balance inside a mountain, estimate its ratio of height to width. Your answer should be very small compared to unity.

****

11.9 T2 Reducing the Elastostatic Equations to Two Dimensions for a Deformed Thin Plate: Stress-Polishing a Telescope Mirror

The world's largest optical telescopes, the two ten meter Keck telescopes, are located on Mauna Kea in Hawaii. It is very difficult to support traditional, monolithic mirrors so that they maintain their figure as the telescope slews, because they are so heavy; so for Keck a new method of fabrication was sought. The solution devised by Jerry Nelson and his colleagues was to construct the telescope out of 36 separate hexagons, each 0.9m on a side. However, this posed a second problem, grinding each hexagon's reflecting surface to the required hyperboloidal shape. For this, a novel technique called *stressed mirror polishing* was developed. This technique relies on the fact that it is relatively easy to grind a surface to a spherical shape, but technically highly challenging to create a non-axisymmetric shape. So, during the grinding, stresses are applied around the boundary of the mirror to deform it and a spherical surface is produced. The stresses are then removed and the mirror springs into the desired nonspherical shape. Computing the necessary stresses is a problem in classical elasticity theory and, in fact, is a good example of a large number of applications where the elastic body can be approximated as a thin plate and its shape can be analyzed using elasticity equations that are reduced from three dimensions to two by the method of moments.

For stress polishing of mirrors, the applied stresses are so large that we can ignore gravitational forces (at least in our simplified treatment). We suppose that the hexagonal mirror has a uniform thickness h and idealize it as a circle of radius R, and we introduce Cartesian coordinates with (x, y) in the horizontal plane (the plane of the mirror before deformation and polishing begin), and z vertical. The mirror is deformed as a result of a net vertical force per unit area (pressure) $F(x, y)$. This force is applied at the lower surface when positive and the upper surface when negative. In addition there are shear forces and bending moments applied around the rim of the mirror.

As in our analysis of a cantilever in Sec. 11.7, we assume the existence of a neutral surface in the deformed mirror, where the horizontal strain vanishes, $T_{\rm ab} = 0$. (Here and below we use letters from the early part of the Latin alphabet for horizontal $x = x^1$, $y = x^2$ components.) We denote the vertical displacement of the neutral surface by $\eta(x, y)$. By applying the method of moments to the three-dimensional equation stress balance $T_{jk,k} = 0$ in a manner similar to our cantilever analysis, we obtain the following two-dimensional equation for the mirror's shape:

$$\boxed{\nabla^2(\nabla^2\eta) = F(x, y)/D\ .} \tag{11.102a}$$

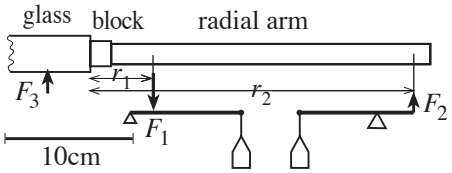

Fig. 11.16: Schematic showing mirror blank, radial arm and lever assembly used to apply shear forces and bending torques to the rim of a mirror in stress polishing. (F_1 need not equal F_2 as there is a pressure F applied to the back surface of the mirror and forces applied at 23 other points around its rim.) The shear force is $S = F_2 - F_1$ and the bending torque is $M = r_2F_2 - r_1F_1$

Here ∇^2 is the horizontal Laplacian, i.e. $\nabla^2\eta \equiv \eta_{,aa} = \eta_{,xx} + \eta_{,yy}$. Equation (11.102a) is the two-dimensional analog of the equation $d^4\eta/dx^4 = W/D$ for the shape of a cantilever [Eq. (11.87)], and the two-dimensional flexural rigidity that appears in it is

$$\boxed{D = \frac{Eh^3}{12(1-\nu^2)}} , \tag{11.102b}$$

where E is the mirror's Young's modulus, h is its thickness and ν is its Poisson ratio. The quantity $\nabla^2\nabla^2$ that operates on η in the shape equation (11.102a) is called the *biharmonic operator*; it also appears in 3-dimensional form in the biharmonic equation (11.29a) for the displacement inside a homogeneous, isotropic body to which surface stresses are applied.

The shape equation (11.102a) must be solved subject to boundary conditions around the mirror's rim: the applied shear forces and bending torques.

The individual Keck mirror segments were constructed out of a ceramic material with Young's modulus $E = 89$GPa and Poisson's ratio $\nu = 0.24$ (cf. Table 11.1). A mechanical jig was constructed to apply the shear forces and bending torques at 24 uniformly spaced points around the rim of the mirror (Figure 11.16). The maximum stress was applied for the six outermost mirrors and was 2.4×10^6N m^{-2}, 12 per cent of the breaking tensile strength (2×10^7N m^{-2}).

This stress-polishing worked beautifully and the Keck telescopes have become highly successful tools for astronomical research.

****

EXERCISES

Exercise 11.22 **** Derivation and Example: Dimensionally Reduced Shape Equation for a Stressed Plate*

Use the method of moments (Sec. 11.7) to derive the two-dimensional shape equation (11.102a) for the stress-induced deformation of a thin plate, and expression (11.102b) for the 2-dimensional flexural rigidity. Here is a step-by-step guide, in case you want or need it:

(a) First show, on geometrical grounds, that the in-plane strain is related to the vertical displacement by [cf. Eq. (11.77)]

$$\xi_{a,b} = -z\eta_{,ab} . \tag{11.103a}$$

(b) Next derive an expression for the horizontal components of the stress, T_{ab}, in terms of double derivatives of the displacement function $\eta(x,y)$ [analog of $T_{xx} = -Ezd^2\eta/dx^2$, Eq. (11.78), for a stressed rod]. This can be done (i) by arguing on physical grounds that the vertical component of stress, T_{zz}, is much smaller than the horizontal components and therefore can be approximated as zero [an approximation to be checked in part (f) below], (ii) by expressing $T_{zz} = 0$ in terms of the strain and thence displacement and using Eqs. (11.34) to arrive at

$$\Theta = -\left(\frac{1-2\nu}{1-\nu}\right) z\nabla^2\eta \ , \tag{11.103b}$$

where ∇^2 is the horizontal Laplacian, (iii) by then writing T_{ab} in terms of Θ and $\xi_{a,b}$ and combining with Eqs. (11.103a) and (11.103b) to get the desired equation:

$$T_{ab} = Ez\left[\frac{\nu}{(1-\nu^2)}\nabla^2\eta\ \delta_{ab} + \frac{\eta_{,ab}}{(1+\nu)}\right] \ . \tag{11.103c}$$

(c) With the aid of this equation, write the horizontal force density in the form

$$f_a = -T_{ab,b} - T_{az,z} = -\frac{Ez}{1-\nu^2}\nabla^2\eta_{,a} - T_{az,z} = 0 \ . \tag{11.103d}$$

Then, as in the cantilever analysis [Eq. (11.80)], reduce the dimensionality of this force equation by the method of moments. The zero'th moment (integral over z) vanishes; why? Therefore, the lowest nonvanishing moment is the first (multiply by z and integrate). Show that this gives

$$S_a \equiv \int T_{za}dz = D\nabla^2\eta_{,a} \ , \tag{11.103e}$$

where D is the 2-dimensional flexural rigidity (11.102b). The quantity S_a is the vertical shear force per unit length acting perpendicular to a line in the mirror, whose normal is in the direction a; it is the 2-dimensional analog of a stressed rod's shear force S [Eq. (11.81)].

(d) For physical insight into Eq. (11.103e), define the bending torque per unit length (bending torque density)

$$M_{ab} \equiv \int zT_{ab}dz \ , \tag{11.103f}$$

and show with the aid of Eq. (11.103c) that (11.103e) *is the law of torque balance* $S_a = M_{ab,b}$ — the 2-dimensional analog of a stressed rod's $S = dM/dx$ [Eq. (11.84)].

(e) Compute the total vertical shearing force acting on a small area of the plate as the line integral of S_a around its boundary, and by applying Gauss's theorem, deduce that the vertical shear force per unit area is $S_{a,a}$. Argue that this must be balanced by the net force density F applied to the face of the plate, and thereby deduce the *law of vertical force balance*.

$$S_{a,a} = F \ . \tag{11.103g}$$

By combining with the law of torque balance (11.103e), obtain the plate's bending equation $\nabla^2(\nabla^2\eta) = F/D$, Eq. (11.102a) — the final result we were seeking.

(f) Use this bending equation to verify the approximation made in part (b), that T_{zz} is small compared to the horizontal stresses; specifically, show that $T_{zz} \simeq F$ is $O(h/R)^2 T_{ab}$, where h is the plate thickness and R is the plate radius.

Exercise 11.23 *Example: Paraboloidal Mirror*
Show how to construct a paraboloidal mirror of radius R and focal length f by stressed polishing.

(a) By comparing the shape of a paraboloid to that of a sphere of similar curvature at the origin, show that the required vertical displacement of the stressed mirror is

$$\eta(r) = \frac{r^4}{64 f^3} \ ,$$

where r is the radial coordinate and we only retain terms of leading order.

(b) Hence use Eq. (11.102a) to show that a uniform force per unit area

$$F = \frac{D}{f^3} \ ,$$

where D is the Flexural Rigidity, must be applied to the bottom of the mirror. (Ignore the weight of the mirror.)

(c) Hence show that if there are N equally-spaced levers attached at the rim, the vertical force applied at each of them is

$$S_{zr} = \frac{\pi D R^2}{N f^3}$$

and the associated bending torque is

$$M = \frac{\pi D R^3}{2 N f^3} \ .$$

(d) Show that the radial displacement is

$$\xi_r = -\frac{r^3 z}{16 f^3} \ ,$$

where z is the vertical distance from the neutral surface, halfway through the mirror.

(e) Hence evaluate the expansion Θ and the components of the strain tensor $\mathbf{\Sigma}$ and show that the maximum stress in the mirror is

$$T_{\max} = \frac{(3-2\nu) R^2 h E}{32(1-2\nu)(1+\nu) f^3} \ ,$$

where h is the mirror thickness. Comment on the limitations of this technique for making a thick, "fast" (i.e. $2R/f$ large) mirror.

****

Box 11.4
Important Concepts in Chapter 10

- **Foundational Concepts**
  - Displacement vector field $\boldsymbol{\xi}$, Sec. 11.2.1
  - Strain tensor $\mathbf{S} = \boldsymbol{\nabla}\boldsymbol{\xi}$, Sec. 11.2.1
  - Irreducible tensorial parts of strain: expansion Θ, rotation R_{ij} and shear Σ_{ij}, Sec. 11.2.2
  - Bulk and shear moduli K, μ; elastic stress tensor $\mathbf{T} = -K\Theta\mathbf{g} - 2\mu\boldsymbol{\Sigma}$, Sec. 11.3.2
  - Molecular origin of moduli and orders of magnitude, Sec. 11.3.4
  - Elastic force on a unit volume, $\mathbf{f} = -\boldsymbol{\nabla}\cdot\mathbf{T} = (K + \mu/3)\boldsymbol{\nabla}(\boldsymbol{\nabla}\cdot\boldsymbol{\xi}) + \mu\nabla^2\boldsymbol{\xi}$ Sec. 11.3.2
  - Elastic force balance, Sec. 111.3.2
  - Elastic energy (energy of deformation), Sec. 11.3.3
  - Connection Coefficients and their use in cylindrical and spherical coordinate systems, Sec11.5
- **Elastostatic Equilibrium**
  - Differential equation for displacement, $\mathbf{f} = 0$ or $\mathbf{f} + \rho\mathbf{g} = 0$, Sec. 11.3.2
  - Boundary condition $T_{ij}n_j$ continuous, Sec. 11.3.2
  - Methods of solving for displacement in full 3 dimensions: separation of variables, Green's functions, Sec. 11.6.2 and Exs. 11.14, 11.15
  - Dimensional reduction via method of moments, and application to rods, beams and fibers, and to plates: Secs. 11.7, 11.9
  - Bifurcation of equilibria: Sec. 11.8

Bibliographic Note

Elasticity Theory was developed in the 19th and early 20th centuries. The classic textbook from that era is Love (1927), which is available as a Dover reprint. An outstanding, somewhat more modern text is Landau and Lifshitz (1986) — originally written in the 1950s and revised in a third edition in 1986, shortly before Lifshitz's death. This is, perhaps, the most readable of all the textbooks that Landau and Lifshitz wrote, and is still widely used by physicists in the early 21st century. Other good texts include Southwell (1941), and Timoshenko and Goodier (1970). For a sophisticated treatment of methods of solving the elastostatic

equations for a body on which external forces act, see Gladwell (1980). For Green's function solutions, see Johnson (1984).

Bibliography

Braginsky, V. B., Gorodetsky, M. L., and Vyatchanin, S. P. 1999. "Thermodynamical fluctuations and photo-thermal shot noise in gravitational wave antennae" *Physics Letters A*, **264**,1.

Braginsky, V. B., Polnarev, A G., and Thorne, K. S. 1984. "Foucault pendulum at the south pole: proposal for an experiment to detect the Earth's general relativistic gravitomagnetic field" *Physical Review Letters* **53**, 863.

Braginsky, V., Mitrofanov, M. and Panov, V. 1984. *Systems with Small Dissipation*, Chicago: University of Chicago Press.

Chandrasekhar, S. 1962. *Ellipsoidal Figures of Equilibrium*, New Haven: Yale University Press.

Gladwell, G. M. L. 1980. *Contact Problems in the Classical Theory of Elasticity*, Alphen aan den Rijn: Sijthoff and Noordhoff.

Jackson, J. D. 1999. *Classical Electrodynamics*, New York: Wiley.

Johnson, K. L. 1984. *Contact Mechanics*, Cambridge: Cambridge University Press.

Landau, L. D., and Lifshitz, E. M. 1986. *Elasticity*, Third Edition, Oxford: Pergamon.

Levin, Yu. 1998. "Internal thermal noise in the LIGO test masses: a direct approach" *Physical Review D*, **57**,659–663.

Liu, Y. T., and Thorne, K. S. 2000. "Thermoelastic noise and thermal noise in finite-sized gravitational-wave test masses" *Physical Review D*, in preparation.

Love, A.E.H. 1927. *A Treatise on the Mathematical Theory of Elasticity*, Cambridge: Cambridge University Press; Reprinted – New York: Dover Publications (1944).

Mathews, J. and Walker, R. L. 1965. *Mathematical Methods of Physics*, New York: Benjamin.

Messiah, A. 1962. *Quantum Mechanics, Vol. II*, North-Holland, Amsterdam.

Misner, C.W., Thorne, K.S., and Wheeler, J.A. 1973. *Gravitation*, W.H. Freeman, San Francisco.

Southwell, R.V. 1941. *An Introduction to the Theory of Elasticity for Engineers and Physicists*, Second Edition, Oxford: Clarendon Press; Reprinted – New York: Dover Publications.

Thorne, K.S. 1980. "Multipole Moments in General Relativity" *Rev. Mod. Phys.*, **52**, 299.

Turcotte, D. L. and Schubert, G. 1982. *Geodynamics*, New York: Wiley.

Timoshenko, S. and Goodier, J. N. 1970. *Theory of Elasticity*, Third Edition, New York: McGraw-Hill.

Will, C. M. 1993. *Theory and Experiment in Gravitational Physics*, Revised Edition, Cambridge: Cambridge University Press.

Yeganeh-Haeri, A., Weidner, D. J. & Parise, J. B. 1992. *Science*, **257**, 650.